

PART III
FUEL CELL RESEARCH
Final Report

[STUDY OF GOLD, PALLADIUM, AND PALLADIUM-GOLD
ALLOY ELECTRODES BY GALVANOSTATIC TECHNIQUES]

by

M. L. Soeder

NASA GRANT NsG-384

FACILITY FORM 602

N 66-81106

(ACCESSION NUMBER)

85

(PAGES)

CR-69264

(NASA CR OR TMX OR AD NUMBER)

(THRU)

None

(CODE)

(CATEGORY)

Alfred University
Alfred, New York

TABLE OF CONTENTS

	Page
INTRODUCTION	1
HISTORICAL	5
EXPERIMENTAL	27
RESULTS AND DISCUSSION	30
The Hydrogen Region	38
Region of Charging of the Double-Layer	50
Region of Oxide Formation	52
SUMMARY OF RESULTS	71
APPENDIX I	72
APPENDIX II	74
APPENDIX III	76
BIBLIOGRAPHY	78

LIST OF TABLES

Table	Page
I Summary of Charging Curve Data on Gold	9
II Comparison of Weight and Atomic Composition of Alloys	27
III Hydrogen Occluded by Palladium and Alloys	45
IV Double-Layer Capacitance Data	51
V Potentials of Principal Anodic Arrests	63

LIST OF FIGURES

Figure		Page
1	Charging Curves for Gold	31
2	Charging Curves for 80% Gold	32
3	Charging Curves for 75% Gold	33
4	Charging Curves for 60% Gold	34
5	Charging Curves for 40% Gold	35
6	Charging Curves for 20% Gold	36
7	Charging Curves for Palladium	37
8	Lower Potential Region of Anodic Charging Curves for Gold	41
9	Anodic Charging Curves for 80% Gold	42
10	Anodic Charging Curves for 75% Gold	44
11	Starting Potentials of Hydrogen Ionization	47
12	Rest Potentials after Interruption of Cathodic Charging	49
13	Cathodic Charging Curves for Gold	54
14	Charging Curves for Gold	58
15	Charging Curve Detail for Palladium	61
16	Charging Curve Detail for 20% Gold	64
17	Charging Curve Detail for 40% Gold	66
18	Charging Curve Detail for 60% Gold	68
19	Typical Anodic Polarization Curve	73
20	Electrolytic Cell	75
21	Electrical Measuring Circuit	77

ABSTRACT

It was the purpose of this research to investigate by the method of galvanostatic charging curves the occlusion of hydrogen and surface oxide formation by a series of palladium-gold alloys. Since palladium and gold form a continuous series of solid solutions, the principal effect of alloying gold with palladium is to change the electronic structure of the d-band of the alloy. At approximately 55 atomic percent gold the d-band becomes full.

It was found that occlusion of electrochemically produced hydrogen was dependent on the alloy having unpaired d-electrons since no occlusion occurred in alloys where unpaired d-electrons are not present. It was also found that the rate of occlusion of hydrogen by the alloys reached a maximum at the 26 atomic percent gold concentration and fell to zero at 62 atomic percent gold.

The results of investigations on electrochemically formed surface oxides are discussed for the alloys, for palladium, and for gold.

INTRODUCTION

It is well known (1) that palladium is able to chemisorb large quantities of hydrogen. Palladium, as a member of the group VIII metals, contains unpaired d-electrons. The chemisorption of hydrogen is postulated as occurring through formation of covalent bonds with the unpaired d-electrons or by donation of electrons to the d-band of palladium (2, 3). Since the d-band in gold is full, it should not be able to chemisorb hydrogen, and indeed it is found inert toward chemisorption of hydrogen up to 0°C. (1). The d-s-electron promotion energy for gold is 3.25 ev.; hence, d-electron promotion and hydrogen chemisorption may be able to occur under more energetic conditions (2).

Gold and palladium exist in face-centered cubic crystals with similar lattice parameters (4). Alloys of the two metals form a continuous series of solid solutions (5), the major difference between the various alloys being the number of electrons in the d-band. Magnetic susceptibility measurements on palladium-gold alloys show that the d-band becomes full at about 55 atomic per cent gold (6).

It was the purpose of this research to investigate the chemisorption and occlusion of hydrogen on palladium, gold, and palladium-gold alloys as a function of the electron composition of the d-band. This investigation was conducted electrochemically by the method of galvanostatic

charging curves. In conjunction with the work on hydrogen, the characteristics of the surface oxides formed during anodic polarization were also studied as a function of alloy composition.

The theory of galvanostatic charging curves is similar to that of polarography (7). According to the Nernst equation, for a reversible cathodic process,

$$E = E^{\circ} - \frac{RT}{nF} \ln \frac{a_R}{a_O}$$

where E° = standard reduction potential

a_R = activity of the reductant

a_O = activity of the oxidant

E = reduction potential (also electrochemical potential) of the reaction occurring at the electrode

when the concentration of the species being reduced falls to zero, the potential becomes increasingly more negative and eventually approaches minus infinity. In practice, there is always another species present to be reduced at a lower potential, so the potential falls only until it reaches a point where another electrochemical reaction supports it. The potential remains nearly constant as long as the reducible species remains. There is a slight, gradual decline in potential as the reaction consumes the oxidant, but not until the concentration of oxidant is seriously depleted will the potential again fall sharply. In aqueous solution, the electrolysis of water will be the

limiting reaction. At the cathode the lowest obtainable electrochemical potential will be that of hydrogen evolution.

The same type of behavior is observed during an anodic process. According to the Nernst equation for a reversible anodic process,

$$E = E^{\circ} - \frac{RT}{nF} \ln \frac{a_O}{a_R}$$

where E and E° are now the oxidation potential and standard oxidation potential, respectively, of the reaction occurring at the anode, the electrochemical potential (which is the negative of the oxidation potential) will become increasingly more positive as the reductant is consumed. The potential will then rise until oxidation of a new species occurs. In aqueous solution the highest positive potential obtainable will be that of oxygen evolution resulting from the electrolysis of water.

For an irreversible electrochemical process, the measured potentials may be displaced to more negative values than for an equivalent reversible process at the cathode and to more positive values at the anode. The amount of displacement will be equal to the overvoltage of the process occurring at the electrode.

To obtain galvanostatic charging curves a constant current is applied to the electrodes and the electrochemical potential is recorded as a function of time or amount of electricity passed. The rising or falling of

the potential with the depletion of oxidizable or reducible species results in the characteristic shape of the charging curves. Each potential plateau represents an electrochemical reaction. Each vertical drop or rise represents a potential range where there is no supporting reaction. A typical galvanostatic charging curve is illustrated in Appendix I.

In addition to electrochemical reactions, another process occurs at the electrode during polarization. This is the charging of the electrical double-layer at the electrode-electrolyte interface (8). When a charge is applied to an electrode, oppositely charged particles arrange themselves next to the electrode. This double-layer of charged particles behaves like a parallel-plate condenser. No current will flow across the double-layer until a sufficient potential difference has been established. During the initial stages of polarization when the potential difference is small and no net charge transfer is occurring, the applied current is all going into the build-up of the potential across the double-layer. Under these conditions, the capacitance of the double-layer at a particular potential may be calculated from the following equation (9)

$$C = I \frac{dt}{dE}$$

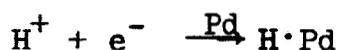
where C = capacitance

I = current density

E = potential

HISTORICAL

It is well known that palladium exothermically absorbs hydrogen in the gas phase (10). An alloy of two phases is formed, a hydrogen poor α -phase and a hydrogen rich β -phase (11). Hoare and Schuldiner (12) found that when palladium was exposed to a hydrogen stirred sulfuric acid solution, the metal absorbed hydrogen to a ratio of 0.025 H/Pd. This was determined to be the α -phase. Its electrochemical potential in 2N sulfuric acid was found to be 0.0495 ± 0.0005 v. vs. the standard hydrogen electrode (SHE). After three hours in the solution, the wire was polarized cathodically and it was found that the hydrogen content rose to 0.63 H/Pd by discharge of hydrogen ion through the reaction



This was determined to be the β -phase. Its electrochemical potential was found to be zero vs. SHE. Flanagan and Lewis (13) found that the β -phase formed spontaneously in hydrogen stirred sulfuric acid in 100 hours.

Aben and Burgers (14), using X-ray diffraction methods, were able to see the α , $\alpha + \beta$, and β -phases on the surface. They postulated high mobility of the hydrogen inside the metal. Norberg (15) studied palladium-hydrogen alloys by NMR and concluded that the hydrogen donated its electron to the d-band of palladium leaving the proton free to move within the metal.

According to Smith (16) absorption or diffusive occlusion of hydrogen does not occur on gold. Ives and Swaroopa (17), however, found that under sufficiently strong conditions atomic hydrogen appeared to be absorbed into the inner structure of gold. They annealed their electrodes in an atmosphere of hydrogen then strongly polarized them cathodically in 0.1 N hydrochloric acid. They feel that gold is normally able to catalyze the recombination of hydrogen atoms leading to the evolution of hydrogen which is usually observed on cathodic polarization; however, annealing in hydrogen was postulated to block active sites on the surface in such a way as to hinder the hydrogen atom recombination reaction. The hydrogen atoms then accumulate at the surface and diffuse into the metal.

Gold and palladium are known to form a continuous series of solid solutions upon alloying (5). Berry (18) measured the amount of hydrogen occluded by several of these alloys of different compositions. It was found that the amount of hydrogen occluded was greatest for pure palladium and fell nearly linearly to zero at the 75% gold alloy.* Sieverts, Jurisch, and Metz (19) found that palladium-gold alloys absorb hydrogen from the gas phase at elevated temperatures forming true ternary alloys. The solubility of hydrogen was found to be greatest in the 40% gold alloy. They found hydrogen

* Unless otherwise stated, all percentages are by weight.

insoluble in the alloys with 50% to 70% gold. More recently, Flanagan and Maeland (20) found that the amount of hydrogen absorbed from a hydrogen stirred hydrochloric acid solution decreased linearly with increasing gold content over the range studied, 5.7% to 31.5% gold.*

Benard and Talbot (21) studied two alloy compositions, 11% and 25% gold, and found no evidence of a two phase system similar to the α - and β -phases of the palladium-hydrogen system. Other workers, however, have found that palladium-gold alloys form α - and β -phases with hydrogen. Mundt (22) found that up to 40% gold a two-phase system was formed. For alloy compositions up to 50 atomic percent gold, Hoare, Castellan, and Schuldiner (23) found that hydrogen was absorbed cathodically to form a two-phase system. They observed that equilibrium potentials of these hydrogen-palladium-gold electrodes fell linearly from 0.05 v. for palladium to 0.0 v. for the 50 atomic percent gold composition.

Surface oxidation of gold has been studied electrochemically by many workers under various conditions. There appears to be general agreement that at least one oxide, of chemical composition Au_2O_3 , is formed on the surface when a gold electrode is polarized anodically from the potential of hydrogen evolution to oxygen

* Weight or atomic percent not stated.

evolution. The electrochemical potential of the $\text{Au}/\text{Au}_2\text{O}_3$ oxidation reaction, which establishes an Au_2O_3 surface layer, has been measured and found to be about 1.36 v. vs. SHE. Formation of lower or higher-valent oxides during anodic charging is in dispute. The considerable variation in results is shown in Table I where a composite summary of the galvanostatic investigations on the oxidation of gold surfaces is given for both perchloric and sulfuric acid electrolytes. A detailed discussion of each work follows.

In 1915 Jeffery (24) was electrolyzing 50% sulfuric acid solution using a gold electrode when he observed that the solution turned green and the gold anode became brown. He attributed the green color to the dissolution of the gold anode and the brown color to the formation of Au_2O_3 and Au_2O on the anode during oxidation. Later Jirsa and Buryanek (25) studied the anodic oxidation of gold in sulfuric acid and concluded that the oxidation occurred in a step-wise process as follows:

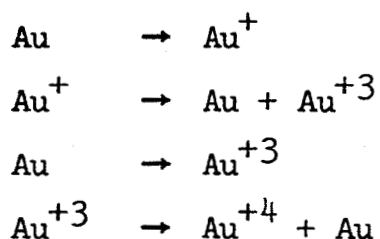


Table I
Summary of Charging Curve Data on Gold

Electrolyte- Electrolyte Atmosphere	Electrode Pretreatment	Polarizing Current $\mu\text{A}/\text{cm}^2$	Potentials of Anodic Breaks in the Charging Curves (vs. SHE)	Potentials of Cathodic Breaks in the Charging Curves (vs. SHE)	Ref.
0.1 N H_2SO_4 (O_2) (N_2)		0.1-1000	1.1 1.27	0.2 0.95	(26)
N H_2SO_4 (N_2)	Wash	5000	1.36	1.0	(27)
0.1 N H_2SO_4	Wash (a)	150 (d)	0.27 0.96 1.26	0.27 1.3	(28)
N H_2SO_4	Cathodic Polar (b)		0.47 0.73 1.13 1.33		(29)
N H_2SO_4 (N_2)		0.5-240	0.4 1.1 1.35	1.2	(30)
N HClO_4	Electro- polish (c)	10-1000	1.28	0.9 1.14	(32)

Table I (continued)

Electrolyte- Electrolyte Atmosphere	Electrode Pretreatment	Polarizing Current $\mu\text{A}/\text{cm}^2$	Potentials of Anodic Breaks in the Charging Curves (vs. SHE)	Potentials of Cathodic Breaks in the Charging Curves (vs. SHE)	Ref.
N HClO ₄	Wash (e)		0.74	0.74 1.24	(33)
N H ₂ SO ₄	Heat air	0.2	0.45 0.7	0.7	(34)
	Heat H ₂ (c)		0.7	0.7	
N H ₂ SO ₄ (N ₂)	Heat O ₂ $\left\{ \begin{smallmatrix} g \\ h \\ c \end{smallmatrix} \right\}$	0.2-8	0.45 0.7	0.45 1.2 0.6 1.2	(35)
N HClO ₄	Heat (i)	2-6000		1.25	(36)
2N H ₂ SO ₄ (O ₂)	Heat (i)	O ₂ oxidation	0.98 1.35		(37)

Footnotes to Table I

- (a) Gold electrolytically deposited on electrode
- (b) C. P. gold
- (c) Spectroscopically standardized gold
- (d) Current density given per electrode
- (e) Mint gold
- (f) Polarization not carried to this portion of the curve
- (g) Fine gold in fresh electrolyte
- (h) Fine gold in initial electrolyte
- (i) Greater than 99.9% pure

Armstrong, Himsworth, and Butler (26) studied the anodic oxidation of gold by the method of charging curves. Working in oxygenated 0.1 M sulfuric acid at current densities in the neighborhood of 10^{-3} to 10^{-7} amp/cm², they found a break on the anodic curves near 1.27 v. which they believed to be the formation of Au₂O₃. The mechanism for the electrochemical formation of this oxide was postulated to involve initially the deposition of a chemisorbed layer of oxygen followed by rearrangement to give Au₂O₃. Following oxygen evolution, the current was reversed and a depolarization process occurred in the charging curve at 0.95 v., corresponding to the reduction of this oxide. Another depolarization occurred at 0.2 v. When oxygen was excluded from the electrolyte, this latter break was absent. Armstrong, Himsworth, and Butler, therefore, concluded that the depolarization step at 0.2 v. was caused by molecular oxygen in the solution. In an oxygenated electrolyte, the anodic charging curves had a second break near 1.1 v. if the previous cathodic polarization was carried below 0.2 v. This step was, therefore, attributed to a reduction product formed on the previous cathodic polarization.

In 1946 Hickling (27) studied the anodic behavior of gold at current densities up to 25 ma/cm² by constant current charging curves. He employed an oscilloscope to obtain traces of the charging curves. The anodic polarization of gold from hydrogen to oxygen evolution was found

to be a two-stage process. The first stage was a rapid linear rise in potential with time and was attributed to the charging of the electrical double-layer. The second stage, beginning at 1.36 v. in normal sulfuric acid, was a slow rise in potential and corresponded to the formation of Au_2O_3 on the surface before oxygen evolution occurred. On current reversal, one cathodic break was found around 1.0 v. Another reduction step was found at a potential slightly more positive than the reversible hydrogen potential and was most clearly seen in neutral solution. The length of this step was dependent on the length of the previous anodic polarization. It was postulated that this step was due to the reduction of an oxidizing agent, possibly molecular oxygen, formed on the previous anodic polarization. This interpretation is in agreement with the work of Armstrong, Himsworth, and Butler (26). Hickling found that the amount of electricity passed in the formation of the oxide was equivalent to 3.4 atoms of oxygen for every 2 atoms of gold on the surface. The quantity of electricity passed on reduction, however, corresponded to only 2.9 atoms of oxygen for every 2 atoms of gold on the surface.

El Wakkad and Shams El Din (28) studied the electrochemical behavior of gold in 0.1 N sulfuric acid by charging curves at very low current densities. They investigated the oxidation of porous gold deposited on a 1 cm^2 platinum foil with currents in the neighborhood of $150 \mu\text{a}$

per electrode. During anodic polarization, potential arrests in the charging curves were found at 0.27, 0.96, and 1.26 v. vs. SHE. Each of these arrests presumably might correspond to the formation of a surface oxide. Various oxides of gold were prepared and equilibrium potentials for gold couples measured in 0.1 N sulfuric acid. The couples and potentials found were Au/Au₂O, E=0.36 v., Au/AuO, E=0.98 v., Au/Au₂O₃, E=1.30 v. in 0.1 N sulfuric acid electrolyte. El Wakkad and Shams El Din felt that the agreement between the equilibrium potentials and the anodic breaks was suggestive that the breaks corresponded to successive formation of Au₂O, AuO, and Au₂O₃. Measurement of the number of coulombs of electricity passed at each stage indicated an oxide two molecules thick in carbonate solution. In acid solution, the film was calculated to be 32 molecules thick in the case of Au₂O. This indicated that Au₂O was somewhat soluble in sulfuric acid. The authors also studied cathodic charging curves and found an arrest corresponding to the reduction of Au₂O₃, at a potential slightly more negative than 1.3 v. They found no evidence of reduction of AuO, but another arrest was found at the Au/Au₂O potential. This step always appeared in neutral or alkaline solutions, but its appearance in acid was dependent upon experimental conditions. The authors agree with Hickling (27) that the step may be the reduction of oxygen formed in the decomposition of Au₂O₃. They proposed that the mechanism for

this reduction of oxygen involves the formation of Au_2O , followed by reduction of this oxide. Potential decay curves from oxygen evolution showed a plateau near the Au_2O_3 potential after which the potential fell, indicating decomposition of Au_2O_3 , to a constant potential more positive than the Au_2O potential. The value of the rest potential suggested that the Au_2O was unstable, decomposing to give gold and Au_2O_3 .

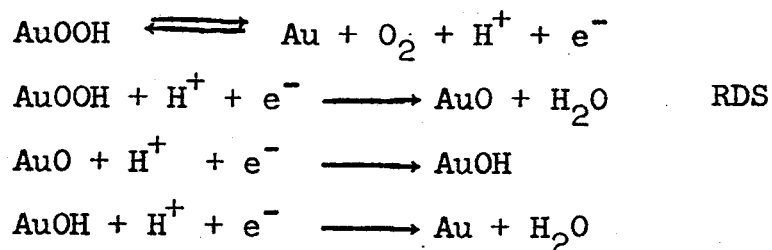
Lee, Adams, and Bricker (29) also found more than one oxide of gold. They observed breaks in the anodic charging curves at 0.47, 1.13, and 1.33 v. in normal sulfuric acid. A slight change in the charging curve slope was found at 0.73 v. The breaks were attributed to the formation of Au_2O , AuO , and Au_2O_3 in agreement with the work of El Wakkad and Shams El Din. The slight change in slope at 0.73 v. was interpreted as being the dissolution of gold. Lee, Adams, and Bricker also noted a plateau beginning at the reversible hydrogen potential on the anodic charging curves. This is in contrast to the results of other investigators and was attributed to the oxidation of surface hydrogen. These authors used long cathodic polarizations as part of the cleaning process prior to running the anodic charging curves. Strong treatment such as this may be responsible for the hydrogen ionization step on anodic oxidation.

Vetter and Berndt (30) studied the electrochemical behavior of gold in normal sulfuric acid at current densities

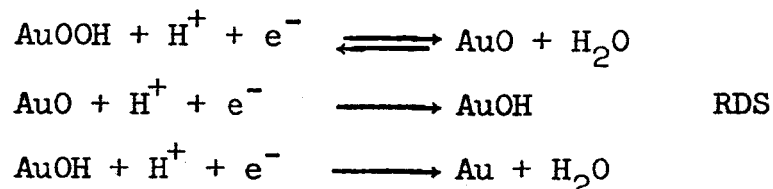
from 0.5 - 240 $\mu\text{a}/\text{cm}^2$. They found two oxides on anodic charging, one at 1.1 v. and one at 1.35 v. A short arrest was observed at 0.4 v. This was believed to be caused by the dissolution of gold. Cathodically, only one reduction step was observed. This was at 1.2 v.

Barnartt (31) working in oxygenated 0.1 M sulfuric acid at current densities around 0.1 ma/cm^2 found that when a clean gold electrode was polarized anodically, the potential rose to 3-5 mv higher than the steady-state potential of about 1.35 v., then fell to the steady-state value. The potential remained constant for 40 hours as the oxide layer thickened. An oxide coating prepared at 0.1 amp/cm^2 for 23 hours was flaked off the electrode and analyzed chemically. The composition was determined to be $\text{Au}(\text{OH})_3$.

Brummer and Makrides (32) studied the surface oxidation of gold cylinders with an apparent surface area of 0.8 cm^2 in molar perchloric acid. The electrodes were cleaned by electro-polishing in a cyanide bath. On anodic polarization, a break in the charging curve was observed at 1.28 v. On cathodic polarization, there were two breaks, one at 1.14 v. and one at 0.9 v. The current densities used were 10-1000 $\mu\text{a}/\text{cm}^2$. No anodic breaks were observed for the formation of lower oxides of gold; however, the existence of these oxides is assumed in the proposed reaction mechanisms for the cathodic process:



This mechanism should be dependent upon the presence of oxygen in the electrolyte, but no such dependence was found. An alternate mechanism proposed by the authors is



They have some reservations about having the decomposition of AuO, whose very existence is doubted by many authors, as the slow step. The authors also noted the zero order decomposition of some active intermediate formed during electrochemical reduction, possibly AuOH, which reacts with water to give oxygen which diffuses away.

Schmid and O'Brien (33) studied the oxygen adsorption and double-layer capacities of gold in normal perchloric acid. They found an anodic and corresponding cathodic step at 0.5 v. vs SCE associated with the adsorption and desorption of a layer of some oxygen containing species, $\text{Au}\cdots\text{O}$ or $\text{Au}\cdots\text{OH}$. A second oxidation-reduction plateau was found at 1.0 v. This was identified as Au_2O_3 .

Deborin and Ershler (34) studied the oxidation of gold electrodes in the potential region between 0.0 v. and 1.0 v.

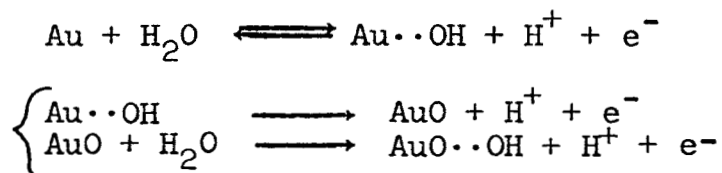
The electrodes were spectroscopically standardized gold wires of 0.72 cm^2 apparent surface area. The electrolyte used was deoxygenated normal sulfuric acid. The electrodes were cleaned in hot aqua regia, rinsed in conductivity water, and heated to 900°C . When the heating was carried out in an atmosphere of hydrogen and the electrolyte saturated with hydrogen, two well-defined depolarization processes were observed on anodic charging at $2.2 \times 10^{-7} \text{ amp/cm}^2$. These processes occurred at 0.4 and 0.7 v. On cathodic charging, only the arrest at 0.7 v. was observed. When the electrodes were heated in the air and the electrolyte flushed with nitrogen, the length of the two anodic arrests became increasingly shorter and eventually disappeared with longer heating times. The arrest at 0.7 v. was attributed to the adsorption of oxygen, and the arrest at 0.4 v. to the desorption of firmly bound hydrogen.

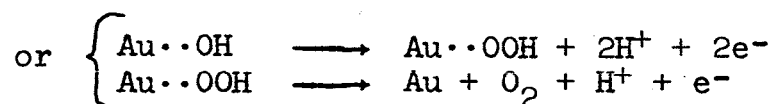
Clark, Dickinson, and Mair (35) felt that the breaks in the charging curves of Deborin and Ershler were a direct result of the heat treatment; therefore, they studied the effect of heating in air, oxygen, and hydrogen on the behavior of gold electrodes. They used electron diffraction, electron microscopy, X-ray emission spectroscopy, and charging curves to study the electrodes. After heating in air or in a stream of hydrogen, only one oxide was found by anodic and cathodic charging curves. This corresponded to Au_2O_3 reported by other workers. After heating in oxygen

at 3 microns pressure, two types of behavior were observed. On the purest samples, spectroscopically standardized gold, the rest potential after heating was 0.45-0.85 v. Cathodic charging indicated that no reducible species were present on the electrode below this potential. On anodic charging at 8×10^{-6} amp/cm² an oxide formed at approximately 1.4 v. and was reduced at 1.2 v. on cathodic polarization. On the less pure electrodes, fine gold, the rest potential was 0.5-0.75 v. after heating in oxygen. Upon reduction at 8×10^{-7} amp/cm², a break occurred at 0.45 v. Anodic polarization in a fresh electrolyte solution (deoxygenated normal sulfuric acid) showed an oxidation step at approximately 1.4 v. The cathodic charging curve had breaks at 1.2 and 0.45 v. In the same electrolyte as the original reduction, an anodic step occurred at 0.65-0.7 v. There was a slight change in slope at 0.45 v. The current was reversed before the formation of Au₂O₃ could begin. On reduction, only one step was observed. This was at 0.6 v. The step at 0.45 v. was missing. The authors attributed the step at 0.7 v. to the Fe(II) / Fe (III) couple. They felt that iron present in fine gold as an impurity migrated to the surface during the heat treatment. This iron must then have dissolved in the electrolyte during the first reduction since the break at 0.7 v. occurred only in the initial solution. On a prereduced electrode in a fresh electrolyte the break did not occur.

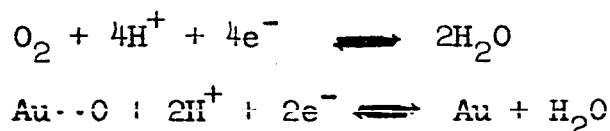
The authors also felt that the break at 0.45 v. was caused by adsorbed hydrogen produced by the reaction of iron with the electrolyte. The reason for the disappearance of the hydrogen reduction step in electrodes not polarized above 1.1 v. was not explained. This step, supposedly caused by iron-produced hydrogen, was also absent in electrolytes to which ferrous sulfate had been added. The authors did not fully explain the reason why electrodes heated in air or hydrogen did not have the break at 0.7 v.

Laitinen and Chao (36) agree with Clark, Dickinson, and Mair that only one oxide of gold is formed and that breaks appearing in charging curves below 1.35 v. are caused by impurities. These authors worked on gold foil (99.9^+ % pure) electrodes of 1 cm^2 area in normal perchloric acid at current densities of $\mu\text{a}/\text{cm}^2$ to ma/cm^2 . The electrodes were heated white hot in an oxygen-natural gas flame to remove the impurities prior to use. The charging curves had no breaks below 1.35 v. The gradually increasing potential which the authors observed on oxidation above 1.36 v. suggested to them that the potential was actually a mixed potential for the formation of oxide plus oxygen evolution. The following mechanism was proposed for the anodic process:





Hoare (37) studied the rest potentials of gold electrodes in oxygenated 2 N sulfuric acid. The electrodes were heated in a hydrogen flame prior to use. After anodization and reduction with hydrogen, the electrode was oxidized by bubbling oxygen through the solution. The potential rose rapidly to 0.6 v., more slowly to 0.8 v., and finally reached a steady potential of 0.98 v. The author felt that this was a mixed potential of the reactions



When oxygen stirring was replaced by nitrogen stirring, this potential fell to 0.78 v. indicating the suppression of the oxygen reaction. Reduction time of the 0.98 v. species corresponded to removal of a monolayer of adsorbed oxygen. Hoare found that on anodic charging a multilayer of hydrated Au_2O_3 was formed. The rest potential of this oxide was found to be 1.35 v. This potential decayed to 0.98 v. both in oxygen and nitrogen stirred sulfuric acid. This behavior indicated the spontaneous decomposition of Au_2O_3 in acid.

The anodic behavior of palladium was studied by Butler and Drever (38) in 1936. They worked with foil electrodes of 1 cm^2 area in dilute sulfuric acid with anodic current

densities of $700 \mu\text{a}/\text{cm}^2$ and cathodic current densities of $5 \mu\text{a}/\text{cm}^2$. The formation of a monolayer of adsorbed oxygen atoms was observed on anodic charging. The reduction of this oxygen was observed on cathodic charging. When the electrode was polarized anodically with a current density of $1 \text{ ma}/\text{cm}^2$, oxide or peroxide of palladium was formed in the neighborhood of 1.4 v. Once this oxide had been formed, it could be reformed anodically at much lower current densities than were necessary for the initial formation. With continued strong anodic polarization the oxide could be made to grow several molecules thick. The authors concluded that a surface oxide could be formed on palladium and that the formation of such an oxide proceeded through adsorbed oxygen atoms.

El Wakkad and Shams El Din (39) studied palladized platinum electrodes of 2 cm^2 apparent area in 0.1 N sulfuric acid which had been deoxygenated. The electrode was polarized cathodically at 2 ma; the current was reversed and reduced to 1 ma. Hydrogen which had dissolved in the spongy palladium electrode on cathodic polarization was oxidized at a potential close to the reversible hydrogen potential. Calculations on the number of coulombs passed at this stage indicated that the H/Pd ratio had been approximately 1/1. After all the hydrogen had been removed from the electrode, the current was reduced to $50 \mu\text{a}$ for the remainder of the charging curve. Following

the oxidation of absorbed hydrogen, a rapid rise corresponding to the charging of the double-layer was observed. The capacitance of the double-layer was $14,175 \mu\text{F}/\text{cm}^2$, indicating a high actual to apparent surface area. Following the charging of the double-layer, two breaks were observed in the anodic charging curve. The first was at 0.85 v. and the second at 1.44 v. The authors concluded that the arrest at 0.85 v. corresponded to the formation of less than a monolayer of $\text{Pd}(\text{OH})_2$. The second arrest was accounted for by the $\text{Pd}(\text{OH})_4/\text{Pd}(\text{OH})_2$ couple. The authors felt that the $\text{Pd}(\text{OH})_2$ was oxidized to $\text{Pd}(\text{OH})_4$ which spontaneously decomposed to give $\text{Pd}(\text{OH})_2$ plus the observed oxygen evolution. Decay from oxygen evolution had a small break at 1.28 v. and became steady at 0.8 v. The cathodic charging curve, however, had breaks at 0.75 and 0.1 v. The species responsible for the latter break was not identified.

Lee, Adams, and Bricker (29) studied palladium foil electrodes of 8 cm^2 area in normal sulfuric acid at current densities of $30\text{-}100 \mu\text{a}/\text{cm}^2$. They agreed with El Wakkad and Shams El Din that $\text{Pd}(\text{OH})_2$ is formed, but at a potential between 0.75-0.77 v. and $\text{Pd}(\text{OH})_4$ is formed between 1.33 - 1.41 v. They proposed that $\text{Pd}(\text{OH})_4$ decomposes leading to oxygen evolution.

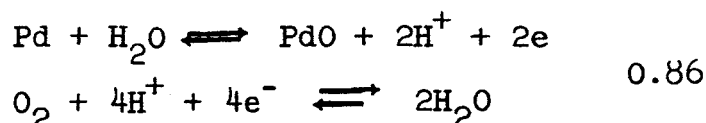
Vetter and Berndt (30) working in normal sulfuric acid at current densities in the neighborhood of $10 \mu\text{a}/\text{cm}^2$ found

that oxygen was chemisorbed on the surface of the palladium electrode at about 0.9 v. This amounted to a monolayer. Cathodically a reduction occurred at about 0.7 v. The amount of electricity passed at this step was only half of that passed anodically at 0.9 v. They attributed this to only partial reduction of the oxygen, to H_2O_2 instead of H_2O . These authors also noted that palladium appeared to be dissolving in the sulfuric acid on anodic charging from 0.8-1.15 v.

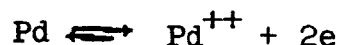
Hickling and Vrjosek (40) studied the behavior of palladium electrodes in deoxygenated normal sulfuric acid with current densities ranging from 0.5-20 ma/cm^2 . Contrary to the results of Vetter and Berndt, they found the same number of coulombs passed in oxidation as reduction at the 0.6-0.8 v. potential plateau. This was equivalent to a layer of $\text{PdO}\cdot\text{H}_2\text{O}$ two to three molecules thick. Anodically, this potential arrest occurred at 0.79 v. and cathodically at about 0.6 v. A second plateau was observed at 1.19 v. anodically and cathodically. The equilibrium potentials of various chemically prepared oxides of palladium were measured in normal sulfuric acid. They are $\text{Pd}/\text{PdO}\cdot\text{H}_2\text{O}$, 0.85 v.; $\text{Pd}/\text{PdO}_2\cdot x \text{H}_2\text{O}$, 1.29 v., and $\text{PdO}\cdot\text{H}_2\text{O}/\text{PdO}_2\cdot x \text{H}_2\text{O}$, 1.23 v. From this they conclude that the second plateau is caused by the formation of $\text{PdO}_2\cdot x \text{H}_2\text{O}$ which accumulates slowly until it is decomposing as fast as it is formed. The potential gradually rises to oxygen evolu-

tion which may take place by way of the decomposition of the higher oxide or accompany its formation. The fact that the higher oxide did decompose was shown by the shortness of its reduction step. The authors also measured the capacitance of the double-layer. The minimum value obtainable was $800 \mu\text{F}/\text{cm}^2$ which they measured in phosphate-buffer electrolyte.

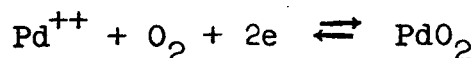
Hoare (41) studied the rest potentials of palladium electrodes in 2 N sulfuric acid. After anodic polarization, the rest potential in oxygenated acid was 1.47 v. On reduction with hydrogen the potential fell to 0.85 v. then finally to 0.05 v. which is the potential of the α -phase, hydrogen-palladium alloy. Oxidation with oxygen caused the potential to rise to 0.87 v. The potential rose above this point only with anodic polarization. Hoare proposed the following sequence of reactions at the electrode:



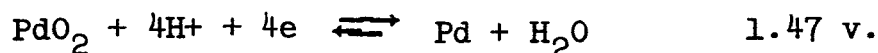
As the potential rises the electrode begins to dissolve.



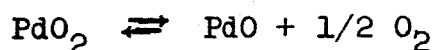
The dissolved Pd can then react with dissolved O_2



but PdO_2 is unstable and decomposes



Oxygen evolution at the Pd/PdO₂ potential is accounted for by assuming that PdO₂, which is formed anodically from PdO, decomposes by the non-electrochemical reaction



When a Pd/PdO electrode was placed in nitrogen stirred sulfuric acid solution, the potential fell to 0.79 v. This indicated to the authors that the 0.86 v. potential was indeed the mixed potential indicated and that the standard potential of the Pd/PdO system could be taken as 0.79 v. The standard potential of the Pd/PdO₂ system was determined by Hoare to be 1.47 v. The difference between this potential and that of Hickling and Vrjosek was noted and explained as being the result of Hickling and Vrjosek's method of preparation of the oxides. Hoare felt that Hickling and Vrjosek were actually measuring the potential of a PdO₂/PdO system created by decomposition of the PdO₂ they were trying to prepare.

Very little work has been done on the anodic behavior of palladium-gold alloys. MacDonald and Conway (42) studied the kinetics of oxygen evolution at palladium-gold alloy electrodes as a function of the composition of the d-band. They found that surface oxide films obscured the role of electronic configuration, but that the behavior of the alloys generally seemed closer to that of palladium than to that of gold.

EXPERIMENTAL

The electrodes studied were made of 0.01 inch diameter wires obtained from Engelhard Industries, Newark, New Jersey. Spectroscopic analysis indicated less than 1 ppm. of any transition metal present as an impurity. The alloy compositions were 80%, 75%, 60%, 40%, and 20% gold by weight. The corresponding atomic percentages are given in Table II. Unless otherwise stated, weight percentages will be quoted in the text.

TABLE II

Comparison of Weight and Atomic Composition of Alloys

Weight Percent	Atomic Percent
80% gold-20% palladium	68.2% gold-31.8% palladium
75% gold-25% palladium	61.7% gold-38.3% palladium
60% gold-40% palladium	44.5% gold-55.5% palladium
40% gold-60% palladium	26.4% gold-73.6% palladium
20% gold-80% palladium	11.9% gold-88.1% palladium

Lengths of wire were cut and sealed into capillary tubing with silastic RTV 502 resin so that 10 cm. of wire was exposed. This corresponded to an apparent surface area of 0.8 cm^2 . The wires were polished with filter paper, wound into a spiral, and cleaned by dipping in dilute, cold hydrochloric acid for 15 minutes. The electrodes were then dipped in distilled water until

ready for use.

The electrolyte used throughout this investigation was normal sulfuric acid (pH 0.3) made from Baker Analyzed Reagent grade sulfuric acid and distilled water. The acid was heated to boiling to expel dissolved oxygen then poured immediately into the electrolytic cell and cooled under an atmosphere of oxygen-free nitrogen (99.995-99.999% pure).

The electrolytic cell, shown in Appendix II, was an all Pyrex U-type with the working and counter compartments separated by a fritted disk. The working compartment contained a gas inlet in the bottom through which the nitrogen was introduced into the cell. This compartment also had a closed top containing a gas outlet and an opening through which the study and reference electrodes were admitted.

The reference electrode was a saturated calomel electrode. The potential of the saturated calomel electrode at 25° C. is 0.242 v. vs. SHE. Through the relationship

$$V_{\text{cal}} + 0.242 = V_{\text{H}}$$

the potentials vs. SCE have all been converted to potentials vs. SHE; therefore, all potentials, unless otherwise stated, are reported vs. SHE. The reference electrode was constructed with a side arm drawn out into a fine capillary which was placed close to the study electrode to minimize ohmic losses. The counter electrode was usually a platinum gauze. For some experiments, a counter electrode identical to the study electrode was used, but

this was found to have no effect on the results.

The electrolytic cell was kept in a constant temperature bath maintained at $25^{\circ}\text{C.} \pm 0.05^{\circ}$. When the electrolyte had cooled to this temperature, the electrodes were introduced into the cell and the nitrogen bubbling was stopped. Leads from a precision constant current generator were clipped onto the ends of the electrodes. The current output was monitored by a Simpson microammeter of 1% accuracy. The potential difference between the study electrode and the reference electrode was monitored by a Corning model 12 pH meter with an input impedance of 10^{14} ohms and ± 5 mv. accuracy. The output of the pH meter was fed into a Varian G-10 graphic recorder. (See Appendix III for electrical apparatus.) The normal chart speed of the recorder was 4 in/min. Current applied to the electrodes on anodic and cathodic polarizations was from $57\text{ }\mu\text{a.}$ to 5 ma. Each electrode was polarized alternately anodically and cathodically a number of times in the course of an experiment. This was effected by means of a reversing switch on the constant current generator.

RESULTS AND DISCUSSION

The general shapes of the charging curves for gold, palladium, and the palladium-gold alloys are shown in Figures 1-7. During a typical anodic polarization of a gold electrode, Figure 1, Curve B, the potential increased sharply from 0.0 v. with the onset of anodic polarization. This rise corresponds to the charging of the electrical double-layer at the electrode-electrolyte interface. Following the charging of the double-layer, a series of step-wise changes in potential occurred as surface oxidations took place. Finally, the potential became fairly steady as oxygen evolution was established. Upon cathodic polarization, Curve C, the potential fell in a step-wise manner as various reduction processes occurred at the electrode. The potential finally became steady at a potential near the reversible hydrogen-electrode potential as hydrogen evolution was established. The general behavior of the 80% gold and the 75% gold alloys was similar to that of pure gold. On palladium and the 60% gold, 40% gold, and 20% gold alloys, there was one additional depolarization step in both the anodic and cathodic charging curves near the potential of the standard hydrogen electrode. This long potential arrest corresponds to charging the electrode with hydrogen before the reversible hydrogen electrode potential was reached on cathodic polarization. At the be-

FIGURE 1 - CHARGING CURVES FOR GOLD ELECTRODES

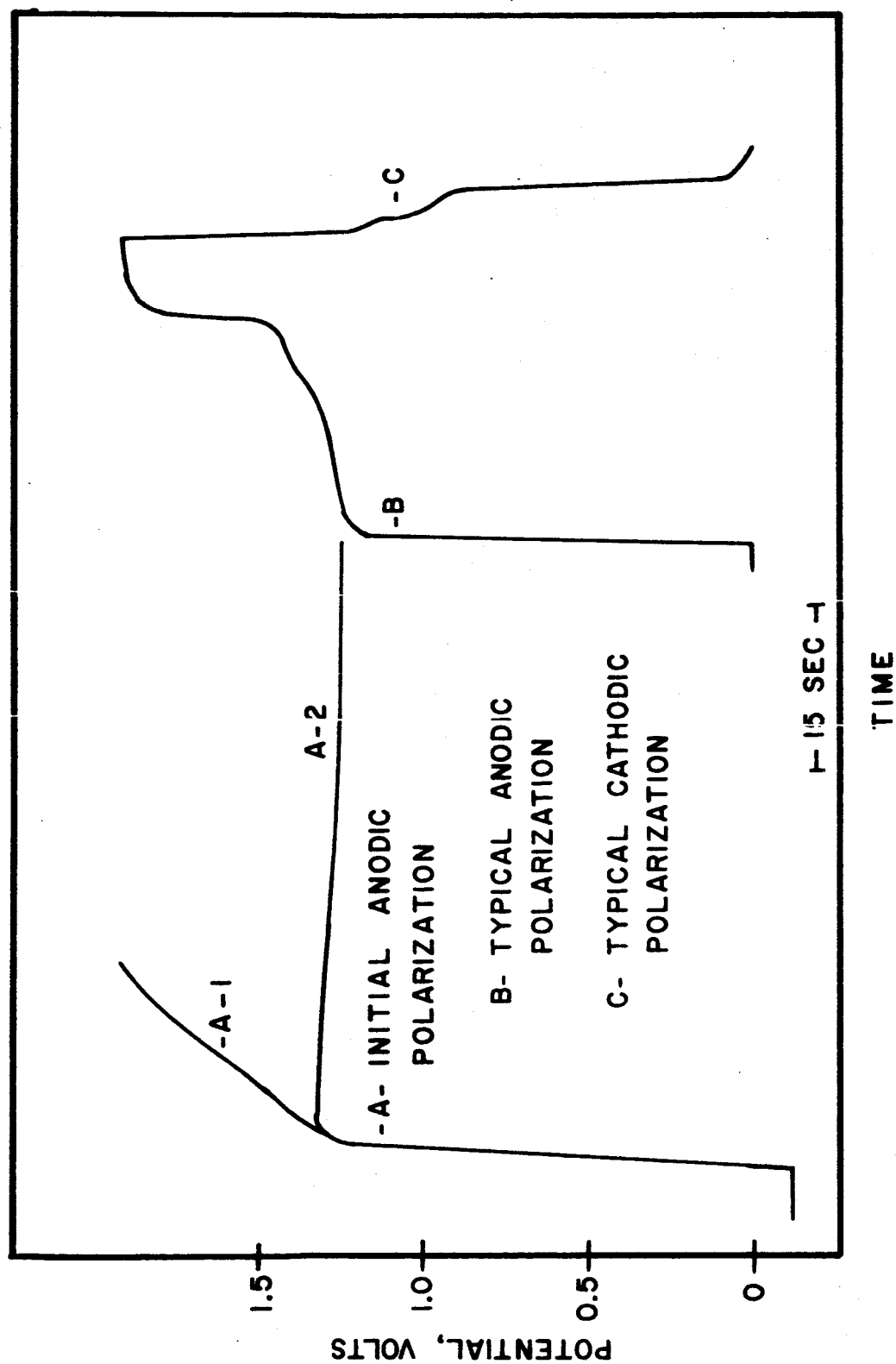


FIGURE 2 - CHARGING CURVES FOR 80% GOLD

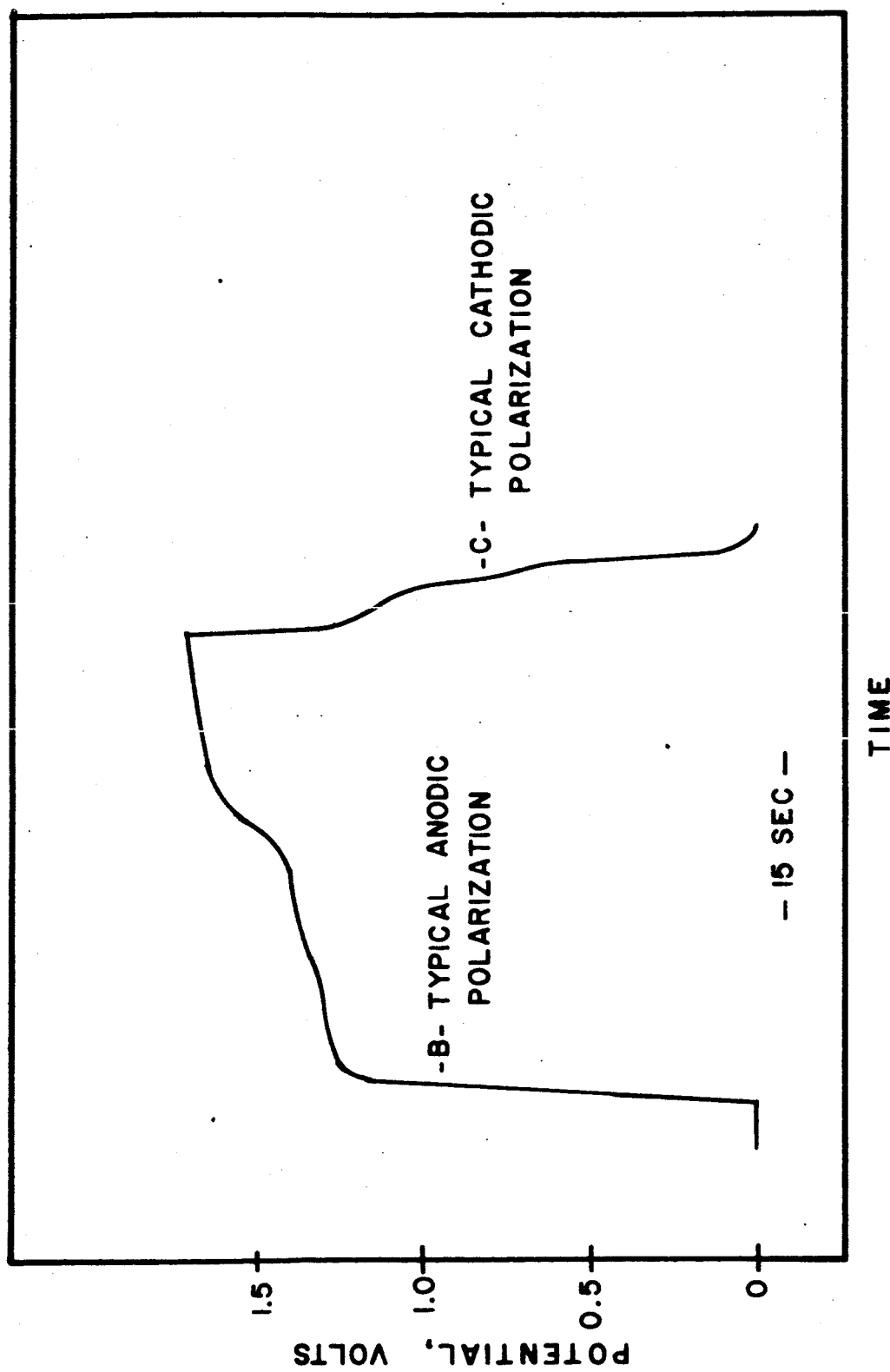


FIGURE 3 - CHARGING CURVES FOR 75% GOLD

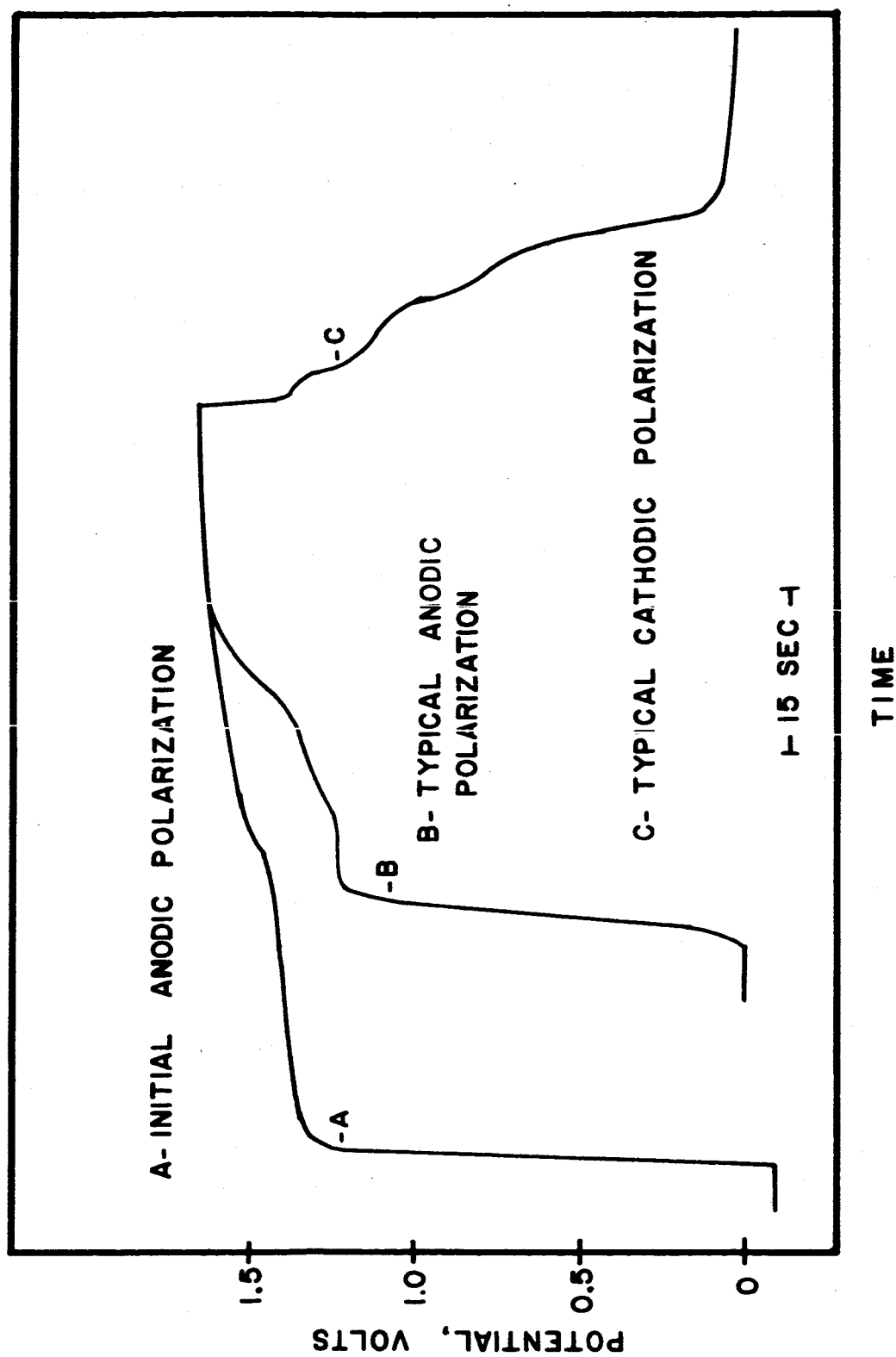


FIGURE 4 - CHARGING CURVES FOR 60% GOLD

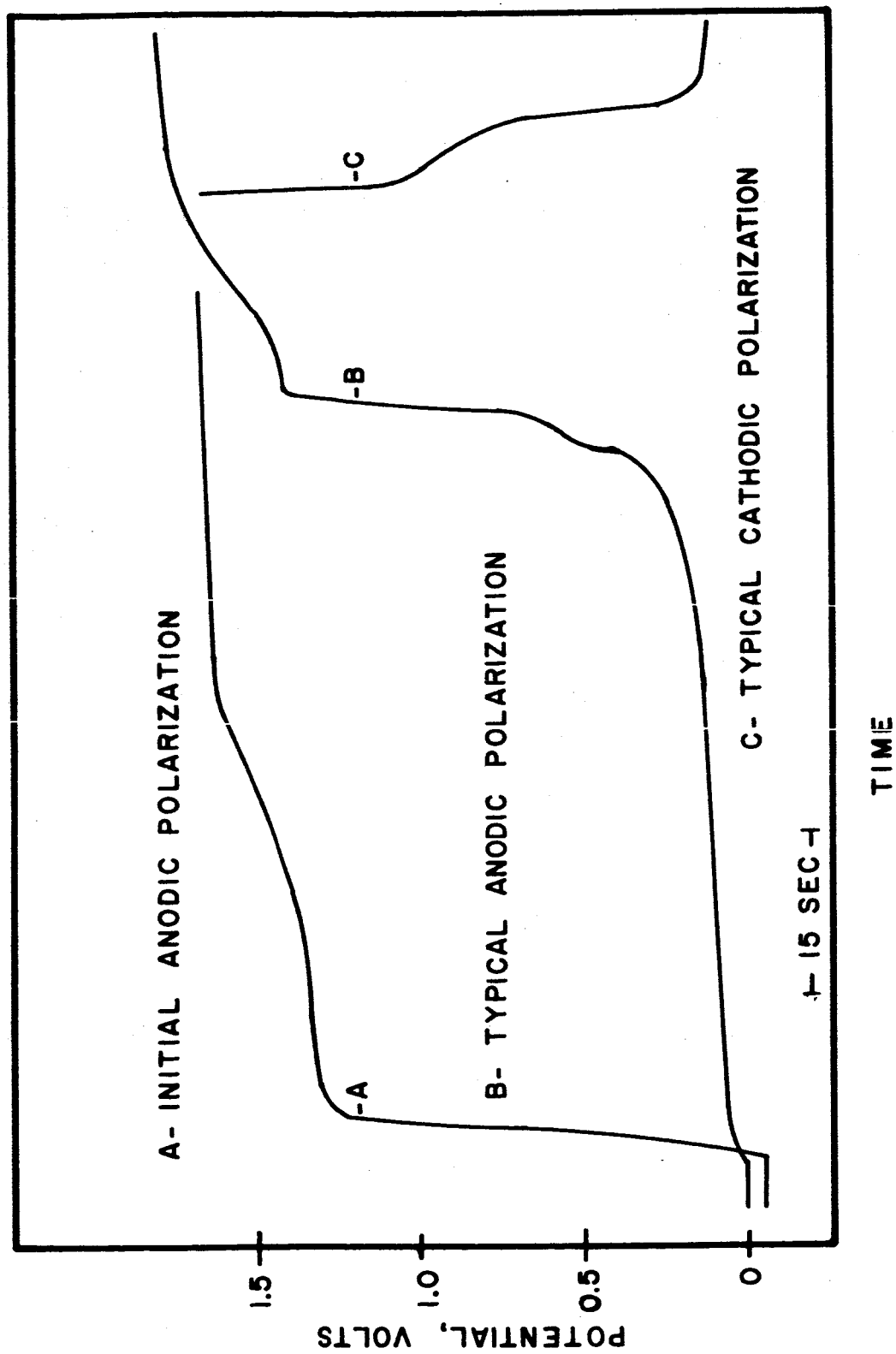


FIGURE 5 - CHARGING CURVES FOR 40% GOLD

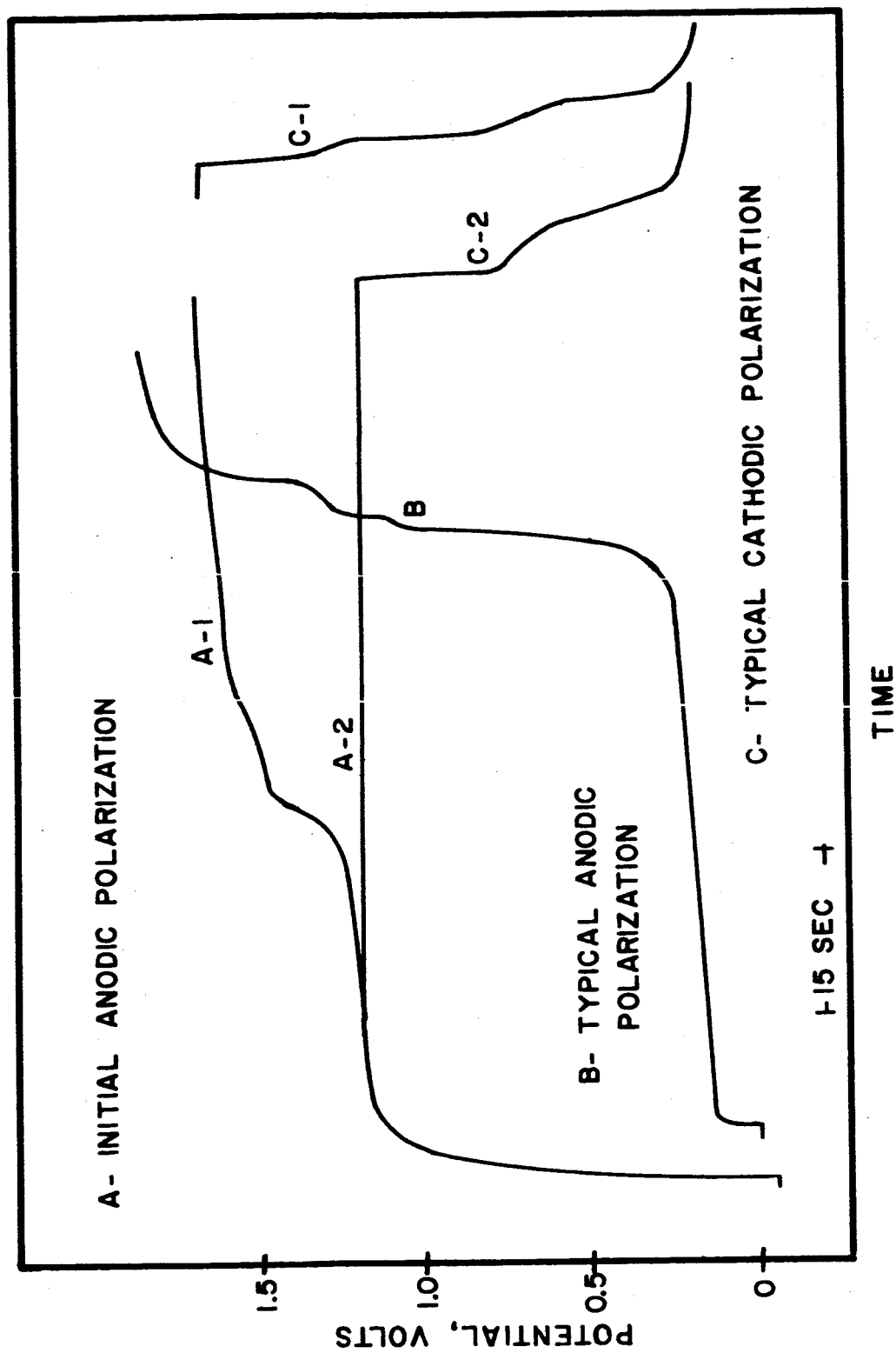


FIGURE 6 - CHARGING CURVES FOR 20% GOLD

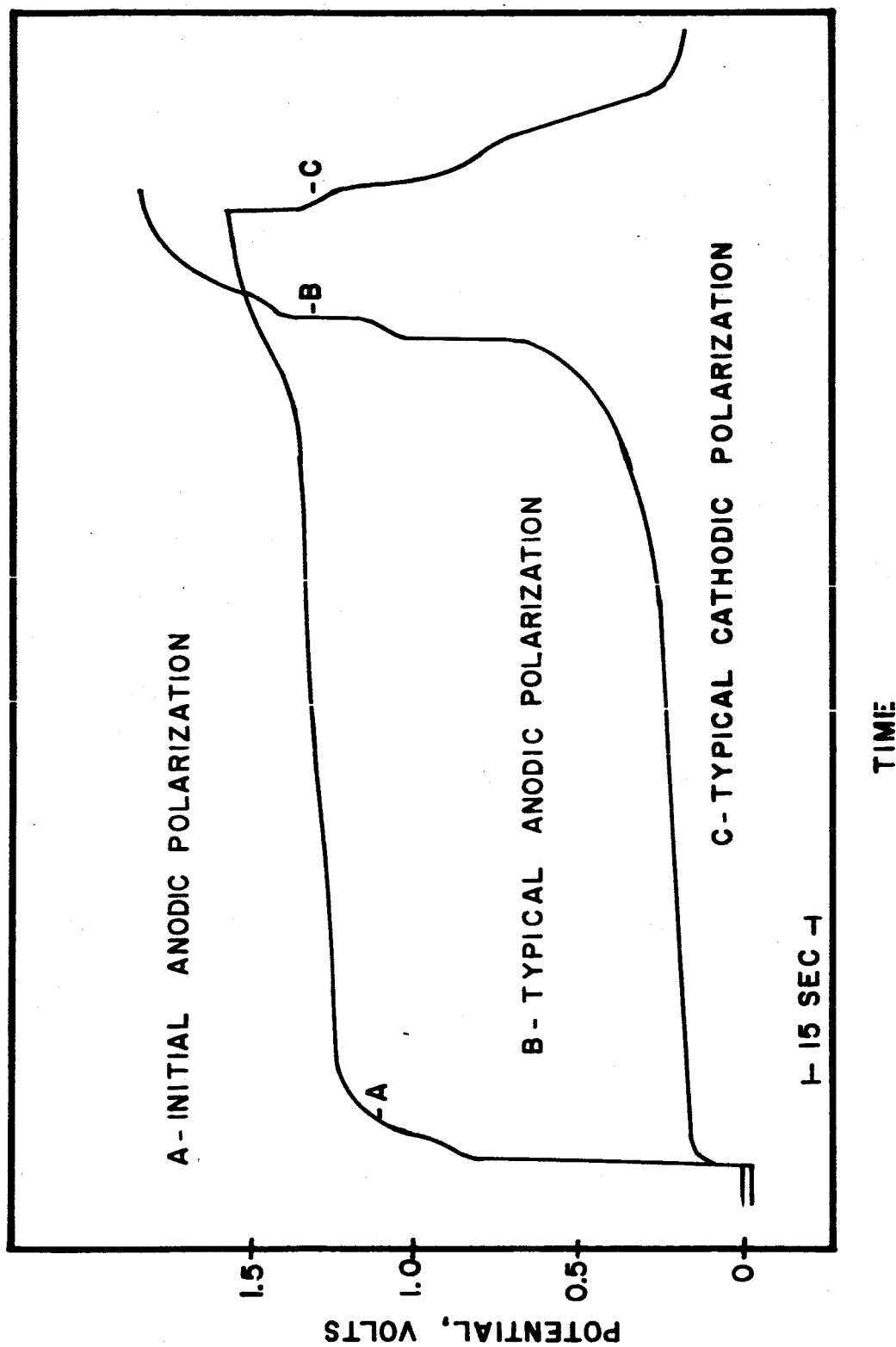
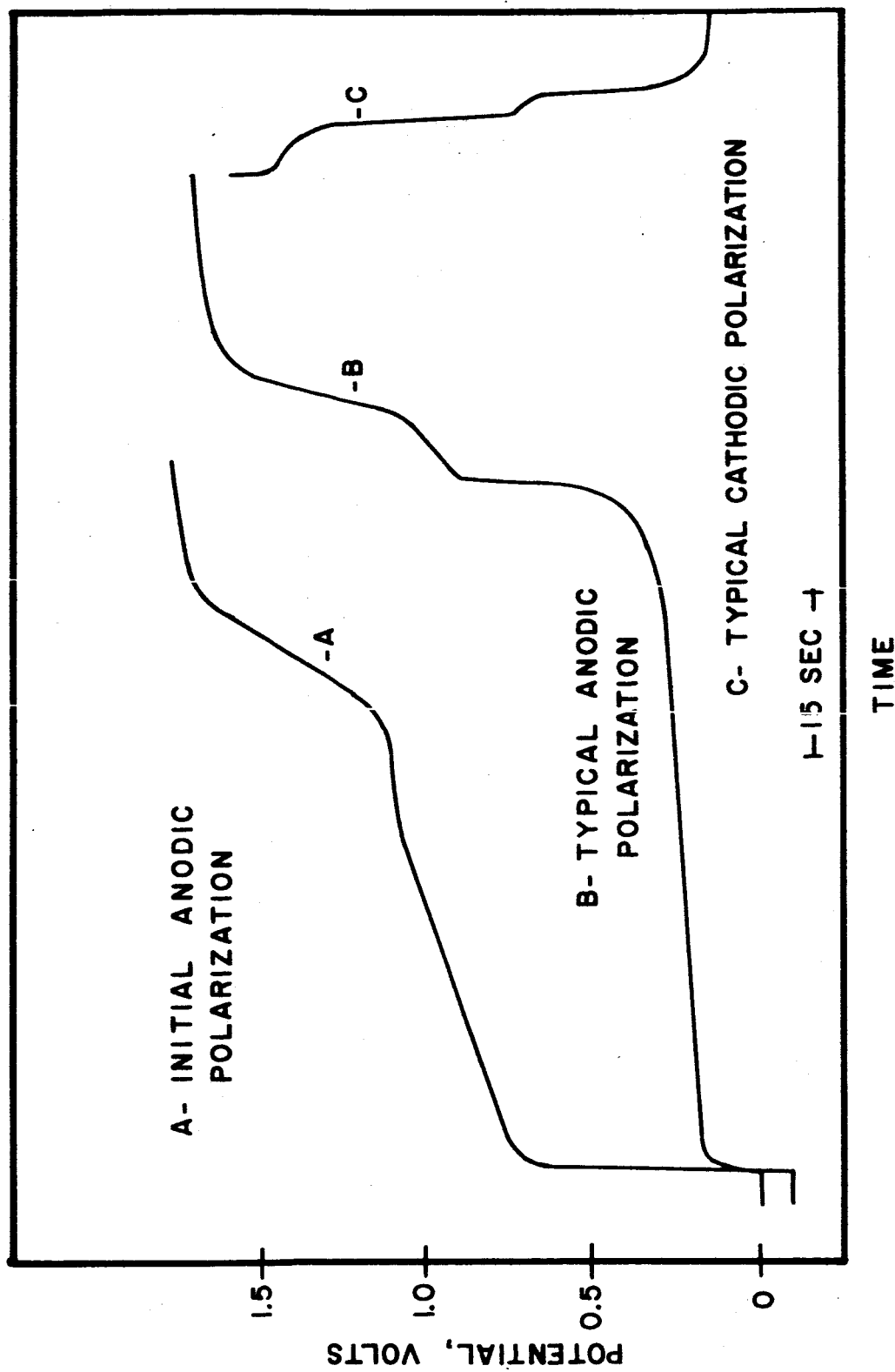


FIGURE 7-CHARGING CURVES FOR PALLADIUM



ginning of anodic polarization, the arrest is the hydrogen ionization step which occurred slightly above the potential of the standard hydrogen electrode.

In Figures 1-7, Curve A is the initial anodic charging curve. It should be noted that in no case was a hydrogen ionization step observed; instead, the potential rose rapidly to the potential of the principal oxide. Apparently the formation of the principal oxide activates the surface toward the chemisorption of hydrogen. After the potential had been raised above that of the principal oxide the subsequent anodic charging curves consistently showed the behavior described in the previous paragraph. A thorough discussion of each region of the charging curves follows.

The Hydrogen Region

Study of the hydrogen region of the galvanostatic charging curves of gold, palladium, and the palladium-gold alloys indicates a drastic change in behavior toward hydrogen occurring at the 75% gold alloy. Palladium electrodes that have been anodically polarized above the potential of the principal oxide are capable of absorbing large quantities of hydrogen. When a palladium cathode from which hydrogen was being evolved was made anodic by reversing the current, the potential immediately rose to a value greater than 30 mv. above the reversible hydrogen-electrode potential. The potential then increased very slowly as hydrogen was desorbed and ionized. The largest

hydrogen oxidation step observed was calculated to correspond to 0.415 coulombs or 2.6×10^{18} hydrogen atoms.

The number of palladium atoms at the surface of the electrode can be calculated from the value of the lattice parameter, 3.88 Å, assuming that the (001) crystal plane is exposed and assuming that the real surface area is twice the apparent area. The latter value is a much-quoted value for a shiny noble metal electrode (27). These calculations indicate that 2.12×10^{15} atoms of palladium are at the surface of the electrode. The ratio of hydrogen atoms, produced through discharge of the ion, to surface palladium atoms is 1225/1. It is apparent from this value that the hydrogen has been absorbed by the electrode. From the density of palladium, 12.16 g/cm³, it was calculated that there are 3.5×10^{20} atoms of palladium in the electrode. The ratio of hydrogen atoms absorbed to palladium atoms present in the bulk is 0.00743/1. Similar behavior in the hydrogen region was noted for the 20% gold, 40% gold, and 60% gold electrodes. Long hydrogen ionization steps on each electrode were observed at potentials somewhat above the reversible hydrogen electrode potential. Electrodes with seventy-five or more percent gold did not similarly occlude hydrogen, Figures 1,2, and 3.

On gold electrodes that had been well cleaned in cold, dilute hydrochloric acid, no hydrogen ionization step was visible in the anodic charging curves. Long cathodic po-

larization, amounting to 16 coulombs, did not cause an anodic hydrogen arrest to occur on clean electrodes, Figure 8, Curve A. On gold electrodes that were cleaned only briefly, a hydrogen ionization step was frequently observed in the anodic charging curve. After adequate cleaning, the step did not appear in the charging curve and did not reappear on later runs. Probably some impurity on the surface of the electrode, and not the gold itself, was responsible for this behavior.

The behavior of the 80% gold alloy is very similar to that of pure gold. Hydrogen does not appear to be absorbed by this alloy. In some cases a small hydrogen ionization step was observed in the anodic charging curves. This step was found to be caused by hydrogen bubble formation at the surface. When bubbles of hydrogen, which were deposited on the electrode during cathodic polarization, were shaken off, the hydrogen ionization step disappeared, Figure 9. At low current densities, however, a very small hydrogen ionization step occasionally remained after the bubbles were shaken off, indicating that a small amount of hydrogen was chemisorbed by the electrode.

The typical anodic charging curve for 75% gold, Figure 3, Curve B, shows a small hydrogen ionization step. Most anodic polarization runs on the 75% gold alloy electrodes indicated some hydrogen ionization. Bubbles were visible on the surface of the electrode, and when they

FIGURE 8 - LOWER POTENTIAL REGION OF ANODIC CHARGING
CURVES FOR GOLD ELECTRODES

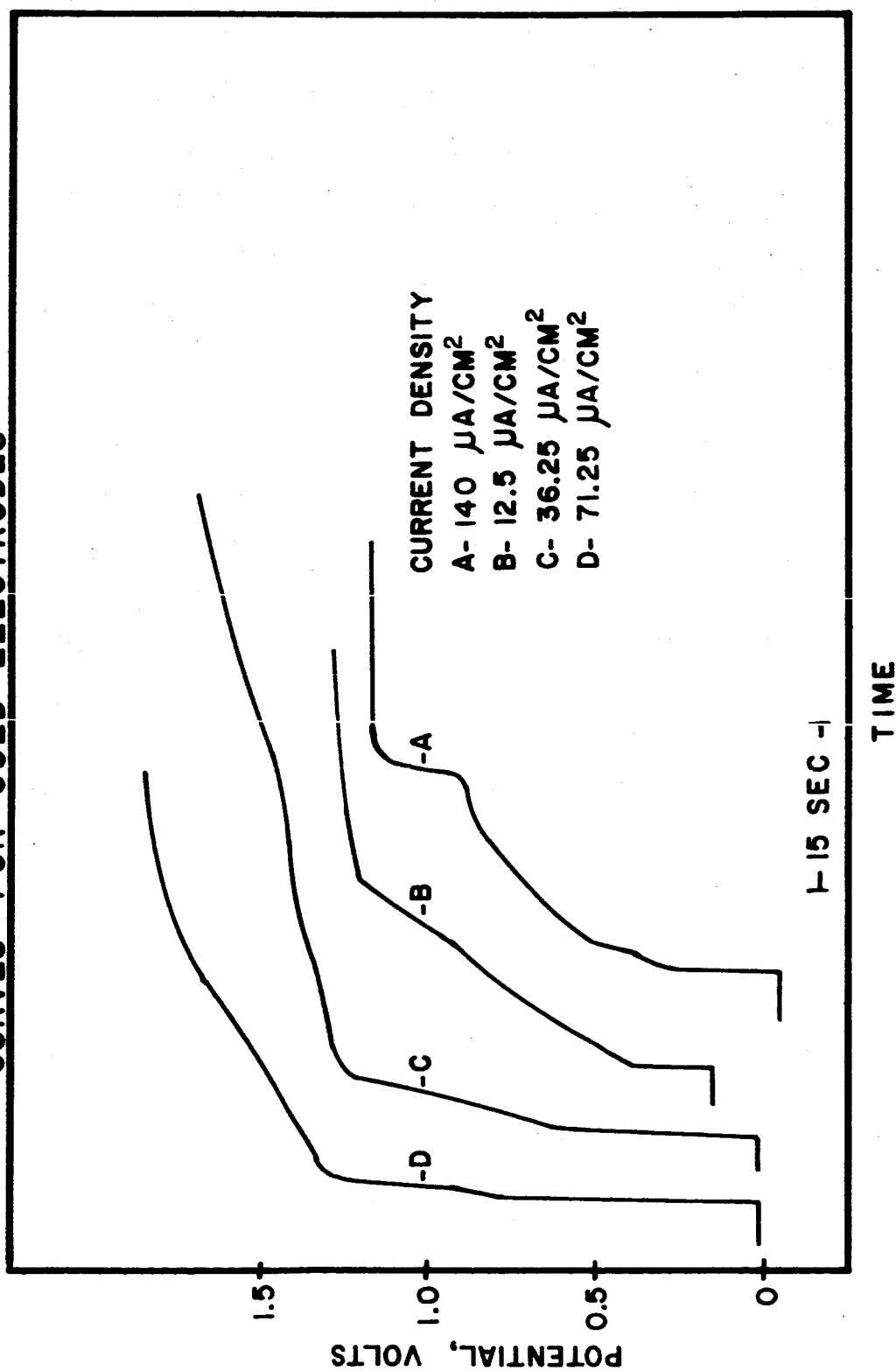
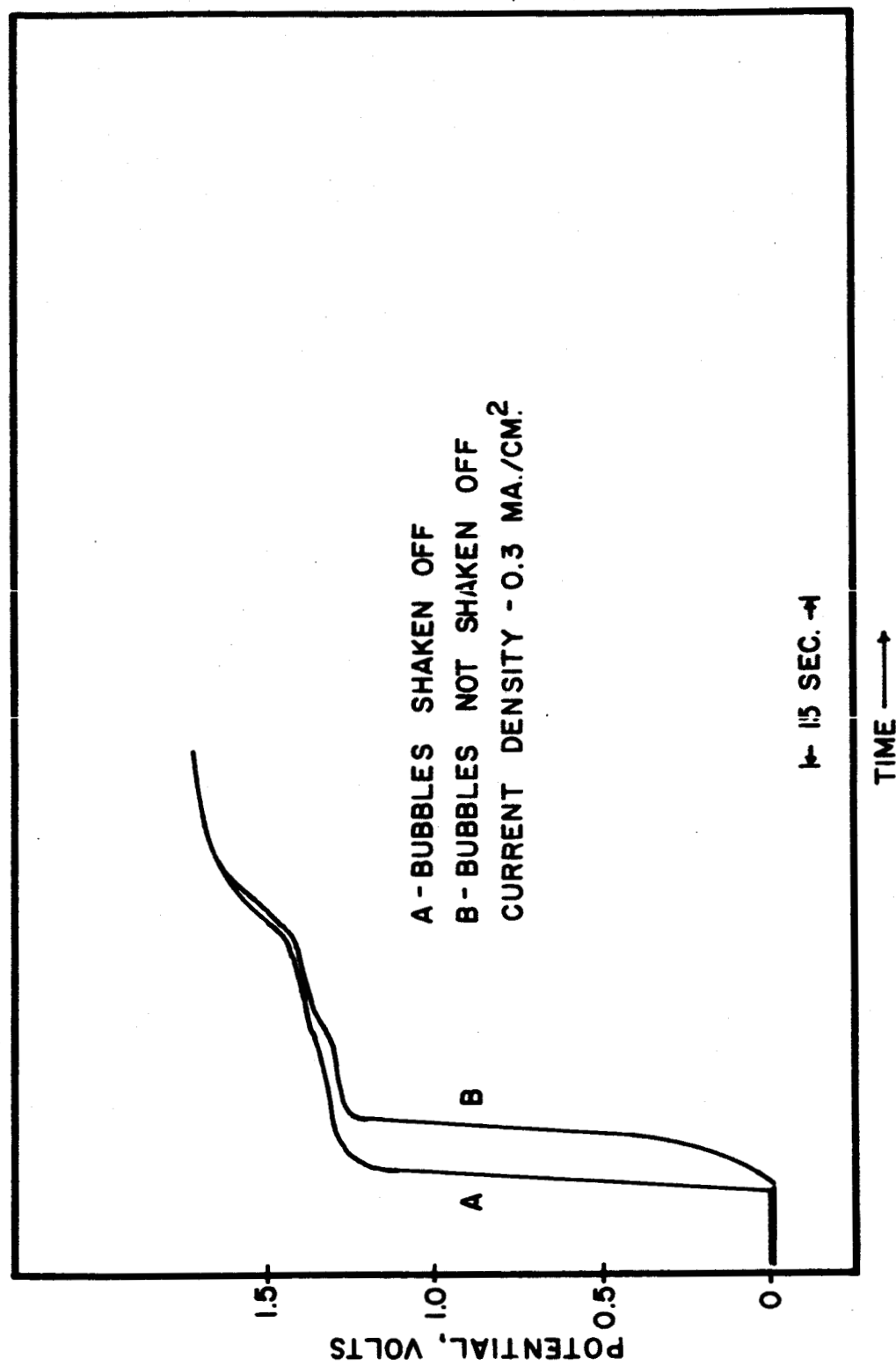


FIGURE 9 - ANODIC CHARGING CURVES FOR 80% GOLD

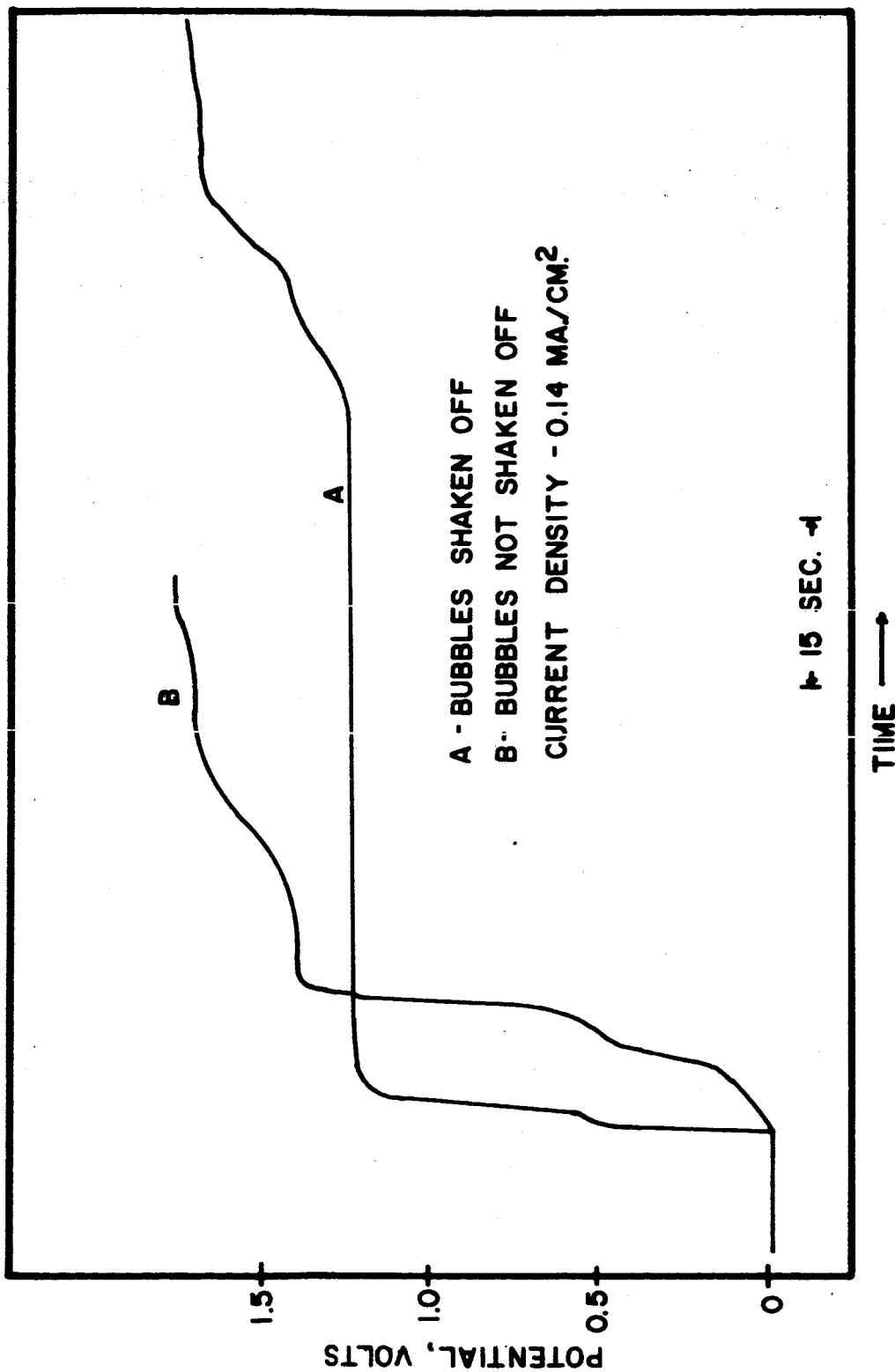


were shaken off, Figure 10, the hydrogen ionization step usually disappeared as with the 80% gold electrode. The fact that small hydrogen ionization steps occurred frequently on the 75% gold alloy, occasionally on the 80% gold alloy, and rarely on gold indicates that alloying even a small amount of palladium with gold may make the surface more active toward chemisorption of hydrogen. Occlusion of hydrogen, however, does not appear to occur on alloys with seventy-five or more percent gold.

Since occlusion of hydrogen is found in the 60% gold alloy but not in the 75% gold alloy, it appears that a change in the electronic structure may be responsible for the change in behavior. At about 75% gold (62 atomic percent) the d-band of the alloys contains no unpaired electrons; whereas, below this gold concentration, unpaired d-electrons are available. This suggests that bonding of hydrogen with unpaired d-electrons is necessary for exothermic occlusion of electrochemically produced hydrogen atoms. Possession of unpaired d-electrons, however, is not a sufficient condition for exothermic occlusion of hydrogen as is illustrated by the fact that many transition metals do not exothermically occlude hydrogen.

During the course of successive anodic and cathodic polarizations, it was noticed that the transition times necessary for cathodic charging with hydrogen to the potential of the standard hydrogen electrode and the anodic removal of this hydrogen were longer for the 40% gold alloy

FIGURE 10- ANODIC CHARGING CURVES FOR 75% GOLD



than they were for the other electrodes. This is demonstrated in Table III where the number of coulombs of electricity passed during the initial hydrogen occlusion step are given for cathodic polarization to the reversible hydrogen-electrode potential. Also included in Table III is the amount of electricity passed anodically during the oxidation of hydrogen absorbed by the electrodes under identical preparative conditions. These values do not represent the maximum amount of hydrogen the electrodes can absorb.


TABLE III

Hydrogen Occluded by Palladium and Alloys

Electrode	Coulombs Required for Initial Hydrogen Ion Discharge	Coulombs Required for Later Hydrogen Ionization
Palladium	0.005	0.0135
20% Gold	0.017	0.3920
40% Gold	0.108	0.5455
60% Gold	0.007	0.0075

It appears that as gold is alloyed with palladium, the rate of hydrogen absorption increases with increasing gold content. This rate appears to reach a maximum near the 40% gold composition after which it decreases rapidly. By the time the gold content of the electrode has been increased to 75%, the absorption ceases. These results may be related

to the work of other investigators who found that certain properties of these and related alloys also pass through maxima in this area*. For example, Nowack (43) found that the occlusive capacity of palladium-silver alloys was maximum around 25% silver; Sieverts, Jurisch, and Metz (19) found that for palladium-gold alloys, gas charged at elevated temperatures, the solubility of hydrogen was greatest in the 26% gold alloy. Couper and Eley (44) reported that the rate of para-hydrogen conversion on palladium-gold alloys was greatest for the 30% gold alloy while Hall and Emmett (45) found that the activity of nickel-copper alloys in hydrogenation of benzene was greatest around

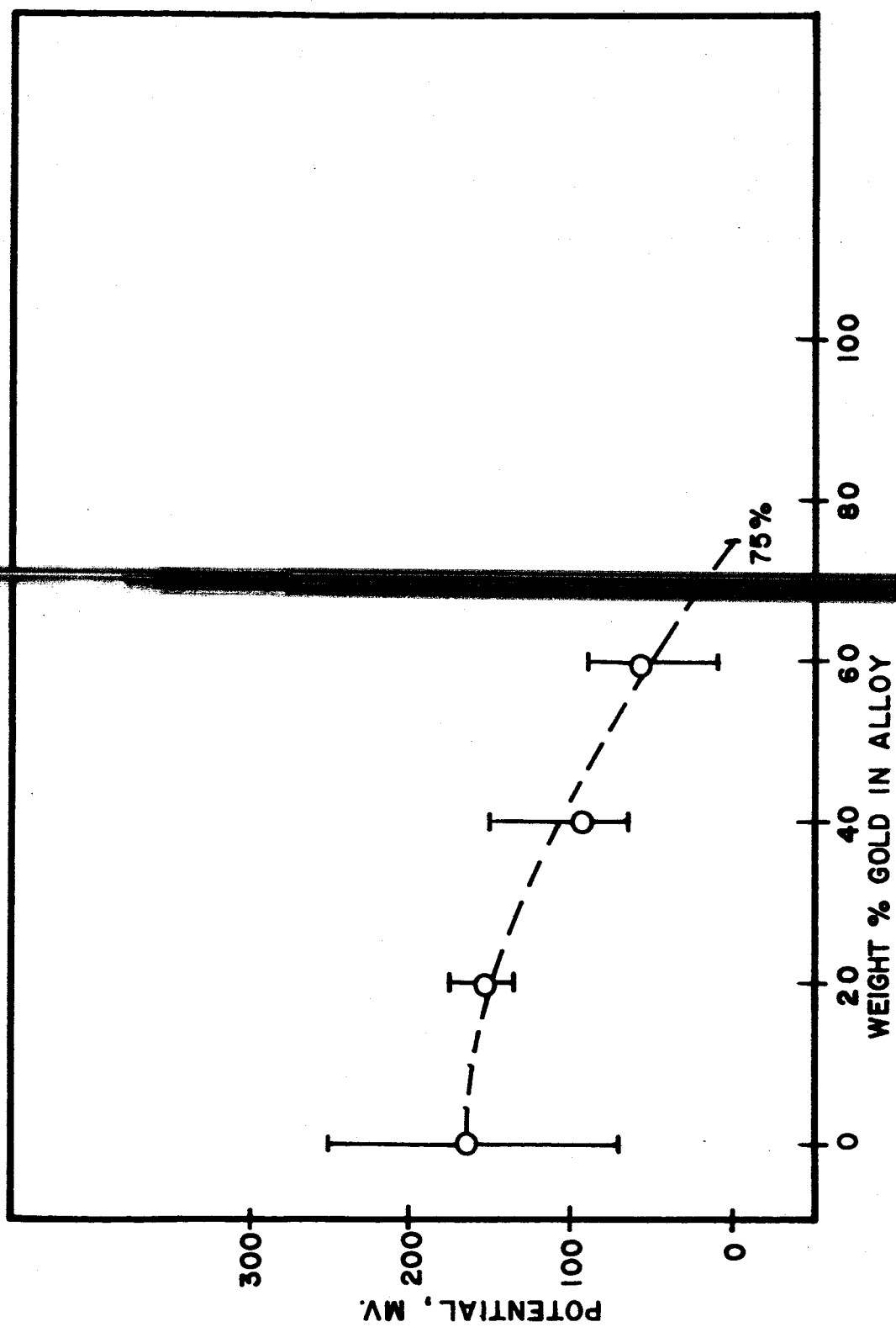


The potential at which hydrogen is anodically ionized at an electrode seems to be a function of several factors. First, the starting potential of the ionization step appears to depend on the composition of the electrode as indicated in Figure 11. The ionization potentials for hydrogen on palladium were generally high, 70-250 mv. For the 20% gold alloy, the values ranged from 135-175 mv. On 40% gold, the values were generally lower, 65-150 mv. while the hydrogen ionization potentials for the 60% gold alloy were between 10-90 mv. Average starting potential values are also shown in Figure 11.

It is difficult to determine experimentally how the potential at which hydrogen begins to ionize anodically

* The following percentages are by atomic composition.

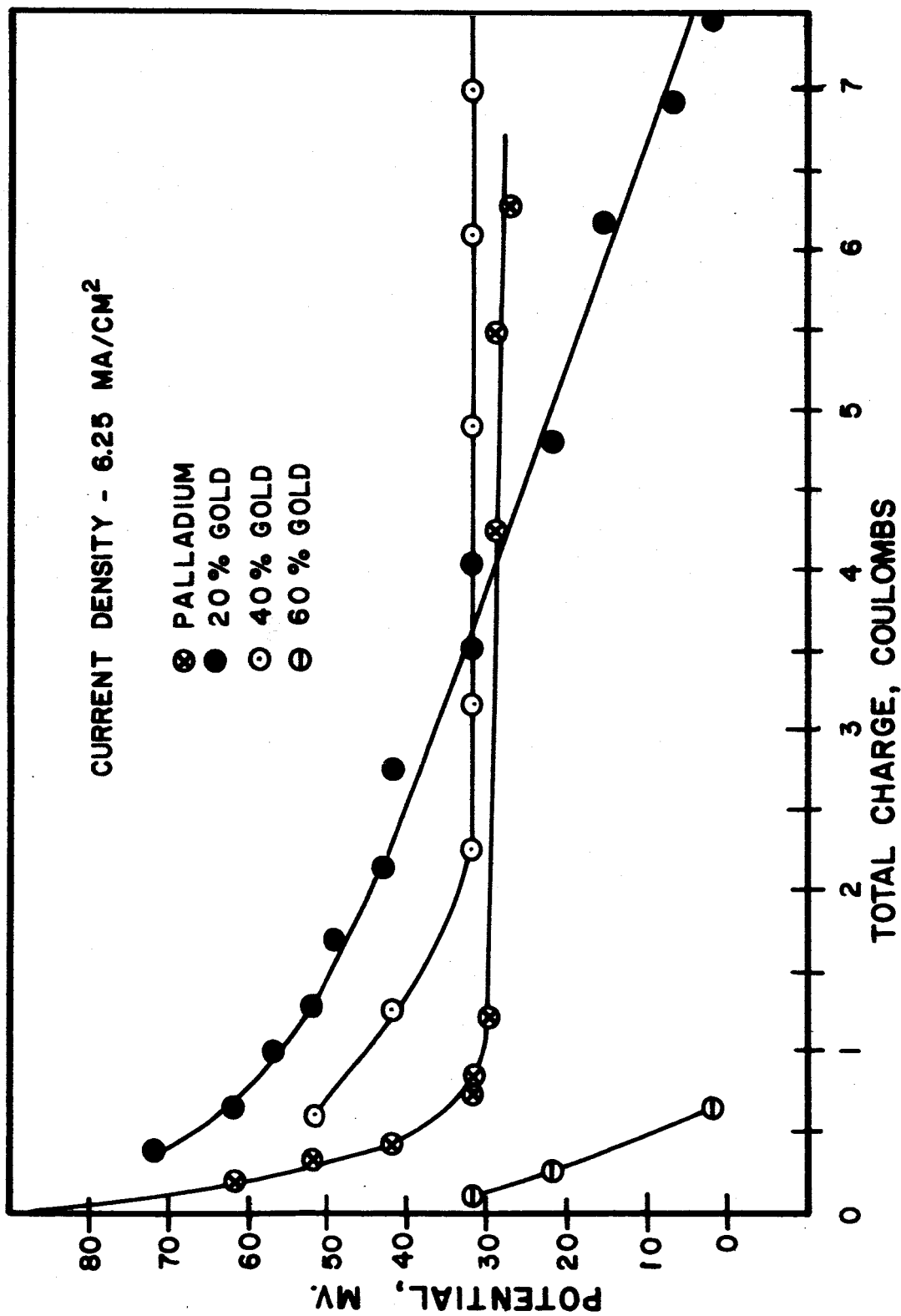
FIGURE 11-STARTING POTENTIALS OF HYDROGEN IONIZATION



varies with polarizing current density. It does appear, however, that hydrogen ionization generally begins at somewhat higher potentials when higher polarizing currents are used.

Another factor which appears to influence the potential at which hydrogen is ionized is the hydrogen content of the electrode. The dependence of potential on hydrogen content is shown in Figure 12. In the experiment, electrodes were polarized cathodically at a current density of 6.25 ma/cm^2 . The circuit was broken periodically and the electrode potential determined. The potentials of the palladium and 40% gold electrodes became stable at 29 and 32 mv., respectively. The coulombs of electricity passed were sufficient to reduce 7.5×10^{18} hydrogen ions at the palladium electrode. This is a hydrogen to palladium ratio of 0.0214/1, a value close to that reported by Hoare and Schuldiner (12), 0.025/1, for the α -phase, palladium-hydrogen alloy whose rest potential is 50 mv. The number of coulombs of electricity passed in order to reach a stable potential in the case of the 40% gold alloy was sufficient to reduce 14.04×10^{18} hydrogen ions. This value corresponds to a hydrogen atom to alloy atom ratio of 0.0418/1 which is within the range of compositions whose potentials would be determined by the α -phase, hydrogen-metal alloy if its behavior toward hydrogen is considered similar to that of palladium. The rest potential is very close to that reported by Hoare, Castellan and Schuldiner (23) for

FIGURE 12 - REST POTENTIALS IN NORMAL SULFURIC ACID AFTER
INTERRUPTION OF CATHODIC CHARGING



a 40% gold-60% palladium electrode that was allowed to absorb hydrogen non-electrochemically from a hydrogen-stirred sulfuric acid solution. The rest potential obtained by them was 35 mv., and it was suggested that the potential-determining species may be an α -phase hydrogen alloy similar to that formed by palladium.

The failure of the 20% gold and 60% gold alloys to reach a stable, positive hydrogen potential can be interpreted to result from the rate of diffusion of hydrogen into both these alloys being slower than the rate of diffusion into the 40% gold alloy. A higher rate for the 40% gold alloy would result in the diffusion of hydrogen into the electrode as fast as the ion is being discharged at the surface. The electrode may then be able to form a fairly homogeneous α -phase hydrogen alloy with a stable positive hydrogen potential. Slower diffusion of hydrogen, formed at the surface at the same rate as for the 40% alloy, would result in an increased hydrogen concentration at the surface of the 20% gold and 60% gold electrodes, thus permitting the formation of a surface state which may be similar to the zero-potential β -phase of palladium-hydrogen.

Region of Charging of the Double-Layer

Between the hydrogen ionization step, when present, and the formation of surface oxides there is a region of rapid linear rise of potential observed during anodic

charging. This is the region in which the electrical double-layer is being charged. For palladium and the three alloys that absorb hydrogen, the capacitance of the double-layer appeared to be abnormally high, apparently due to some continued ionization of hydrogen into the double-layer region. Table IV shows the minimum values of the capacitance of the double-layer calculated from charging curve data for palladium, 20% gold, 40% gold, and 60% gold. For gold and the 75% and 80% gold alloys, the average value of the capacitance of the double-layer is given.

TABLE IV

Double-Layer Capacitance Data

Electrode	Capacitance of the Double-Layer	Current Density
Palladium	2133 $\mu\text{F}/\text{cm}^2$	2.5 ma/cm^2
20% Gold	4210 $\mu\text{F}/\text{cm}^2$	6.25 ma/cm^2
40% Gold	7075 $\mu\text{F}/\text{cm}^2$	6.25 ma/cm^2
60% Gold	637 $\mu\text{F}/\text{cm}^2$	1.25 ma/cm^2
75% Gold	396 $\mu\text{F}/\text{cm}^2$	0.14 ma/cm^2
80% Gold	295 $\mu\text{F}/\text{cm}^2$	0.14 ma/cm^2
Gold	225 $\mu\text{F}/\text{cm}^2$	0.14 ma/cm^2

For all the electrodes, the capacitance of the double-layer was much lower on the initial anodic polarization. The initial values ranged from 117 to 184 $\mu\text{F}/\text{cm}^2$ at 0.14 ma/cm^2 . The values of the capacitance of the double-layer for the initial anodic polarizations are near the values reported by Armstrong, Himsworth, and Butler (26), 110 $\mu\text{F}/\text{cm}^2$, and by Hickling (27), 150 $\mu\text{F}/\text{cm}^2$, for gold electrodes. Laitinen and Chao (36), using more sophisticated methods, have obtained values for the double-layer capacitance of 50-60 $\mu\text{F}/\text{cm}^2$. That the values for the double-layer capacitance are higher after the electrode has been oxidized is an indication that formation and subsequent reduction of surface oxides may temporarily enlarge the actual surface area which is exposed to the electrolyte.

Region of Oxide Formation

After the electrochemical ionization of hydrogen, when present in the electrode, one to four additional depolarization steps were observed during anodic polarization to oxygen evolution. Usually only one or two steps was observed; however, repeated anodic-cathodic cycling and lowered current density, at times, gave rise to additional arrests in the charging curves.

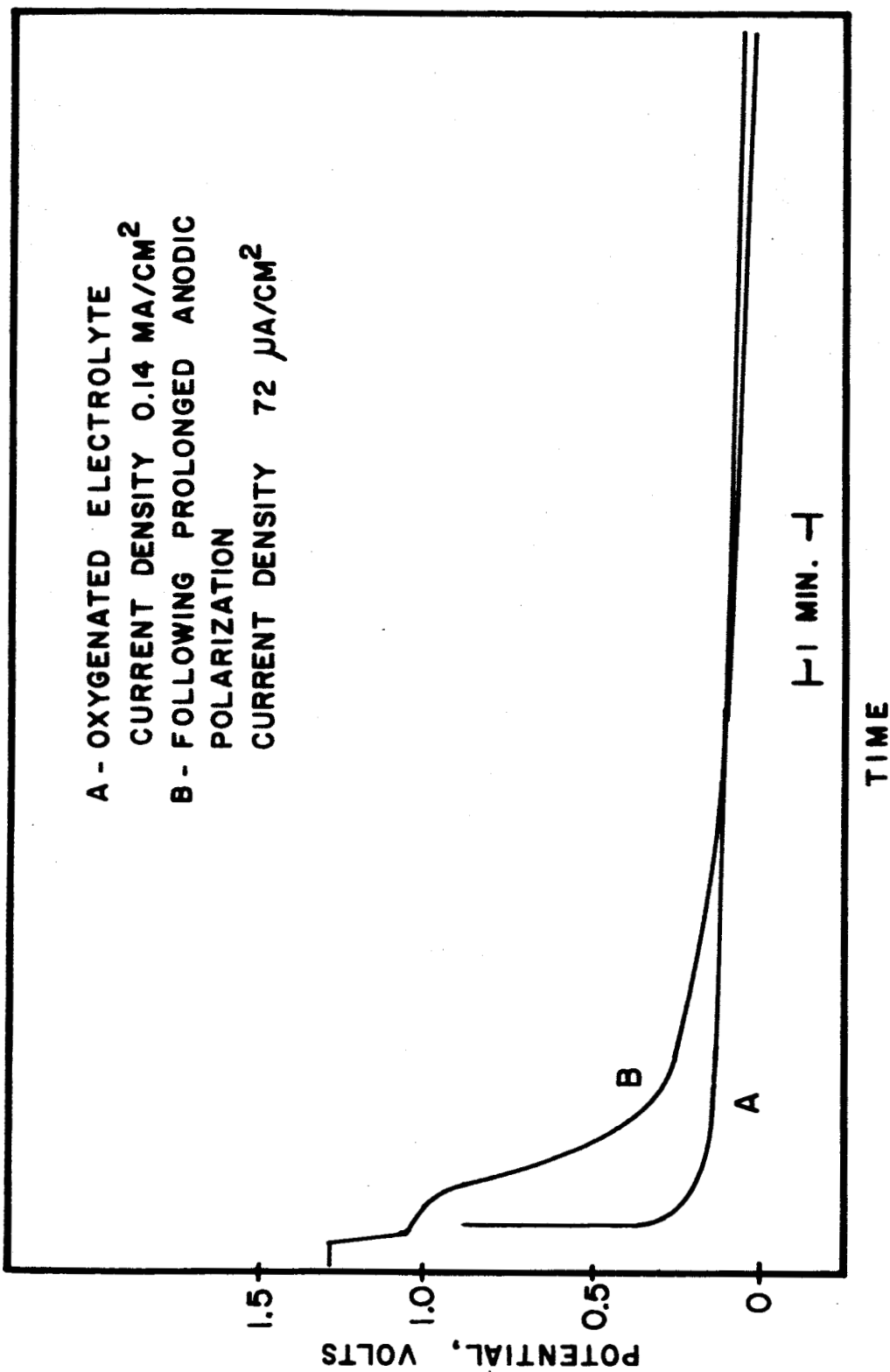
Anodic charging curves of gold indicated that surface oxidation was step-wise, the two principal steps occurring at approximately 1.26 v. and 1.38 v. One or

the other step, but not both together, has been reported by earlier workers and the potential identified with the formation of Au_2O_3 . The two steps frequently merged into one beginning at a potential of approximately 1.26 v.

At other times the first step was bypassed completely and no depolarization step was visible before 1.38 v. With repeated anodic-cathodic cycling both steps became well defined.

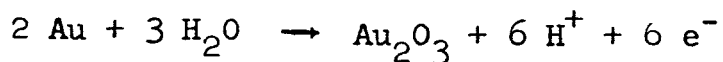
On the initial anodic polarization, Figure 1, Curve A, the potential rose to 1.38 v. then after a short pause, either continued to rise to oxygen evolution, Curve A-1, or fell to 1.26 v., and remained constant there, Curve A-2. The coulombs of electricity and transition times associated with the anodic process occurring at 1.26 v. on any polarization were extremely variable. On several occasions the potential was maintained for nearly 24 hours with no indication that it could not be maintained for considerably longer. After the first few hours, a yellow color began to develop in the electrolyte. A few drops of the electrolyte imparted a grey-pink color to mercurous chloride, indicating the presence of gold in the electrolyte. When the current was reversed after 3 coulombs had been passed at 1.26 v., the potential did not fall quickly to the potential of hydrogen evolution but remained somewhat more positive for several minutes. Figure 13 shows the similarity of this behavior, Curve B, to that of a gold electrode

FIGURE 13 - CATHODIC CHARGING CURVES FOR GOLD



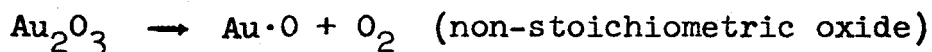
polarized cathodically in an oxygenated sulfuric acid electrolyte, Curve A. This indicates that in addition to gold, molecular oxygen was introduced into the electrolyte during the prolonged anodic polarization at 1.26 v. The reaction occurring at 1.26 v., however, was found to be independent of the concentration of oxygen in the electrolyte. This indicates that oxygen is not involved in the electrochemical reaction that determines the potential. Hydrogen was also bubbled through the electrolyte and found to have no effect on the potential of this reaction. The presence of hydrogen in the electrolyte, however, did make it possible to sustain the potential of this reaction at somewhat higher current densities than usual.

The absolute identification of the potential-determining reactions at 1.26 v. and 1.38 v. was not possible by the methods employed; however, the following mechanism is one that accounts for the observations made. The potential of the Au/Au₂O₃ couple has been reported as 1.36 v. by several investigators, (27, 37), and it is proposed that the electrochemical reaction occurring at this potential is indeed:

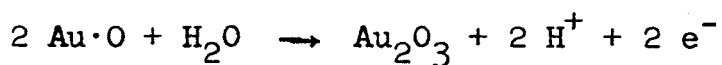


The oxide may be hydrated or exist as Au(OH)₃. It has been noted by others that this oxide decomposes in acid solution (37). Decay curves substantiate this instability

since the potential on decay does not remain at 1.36 v. but falls to a value around 1.0 v. It therefore seems reasonable to assume that some of the Au_2O_3 might decompose immediately after its formation. If the chemical decomposition of Au_2O_3 can be represented as



a surface of chemisorbed oxygen would be produced from the decomposition. This surface could then undergo electrochemical oxidation to Au_2O_3 through the following mechanism:



The sum of these two reactions results in the production of oxygen, the potential-determining reaction being the formation of Au_2O_3 from a layer of chemisorbed oxygen. This latter mechanism for oxidation is similar to that suggested by Armstrong, Himsforth and Butler (26).

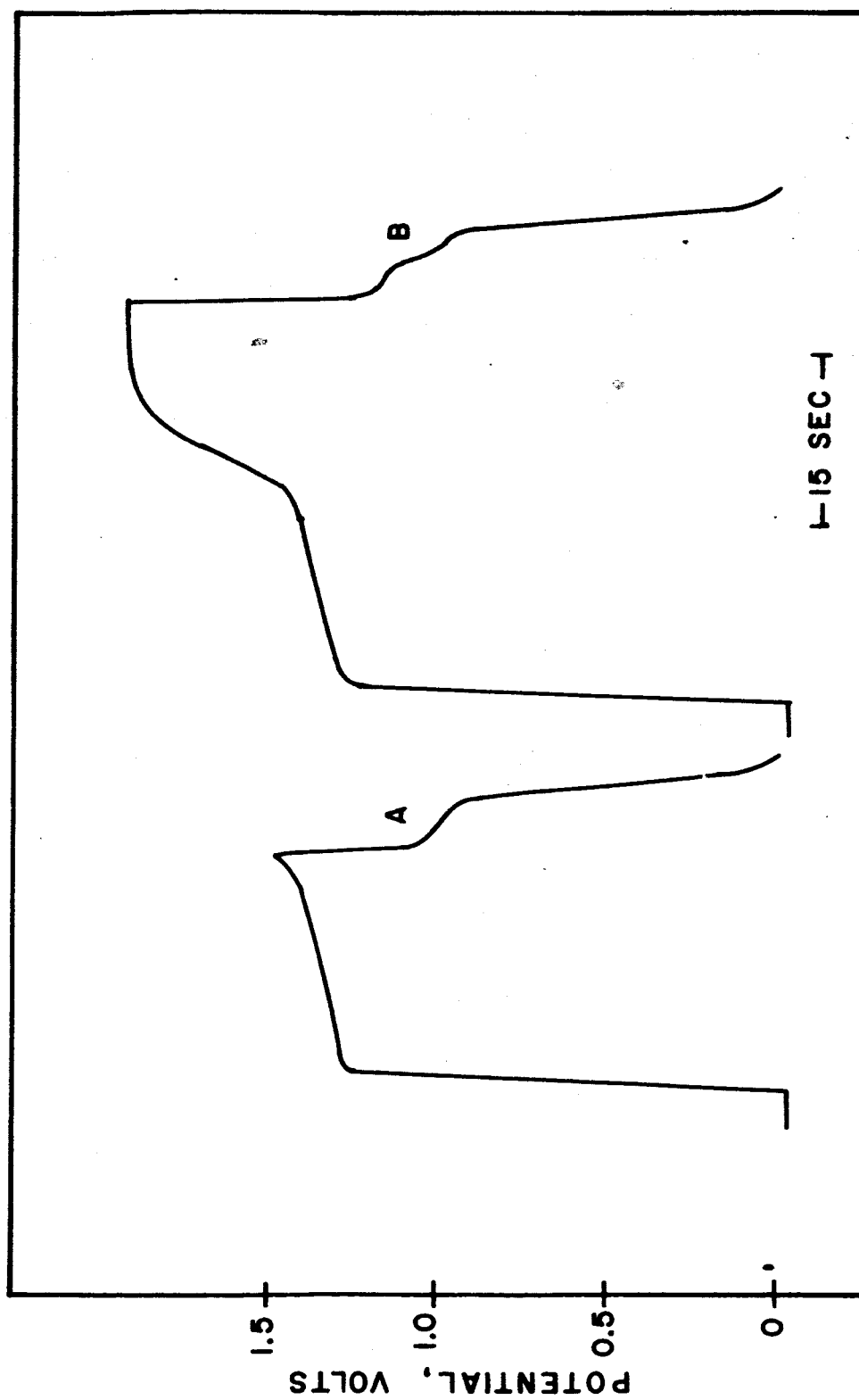
On the initial anodic polarization there is no layer of chemisorbed oxygen and, hence, the potential is determined by the $\text{Au}/\text{Au}_2\text{O}_3$ couple alone. This potential cannot be maintained and must either rise to oxygen evolution or drop to the proposed $\text{Au}\cdot\text{O}/\text{Au}_2\text{O}_3$ potential, 1.26 v. The presence of hydrogen in the electrolyte presumably assisted in the chemical reduction of Au_2O_3 . Since each gold species regenerates the other, the 1.26 v. potential should be able to be sustained considerable periods of time and

there should be no large build-up of oxide on the electrode at this potential. Cathodic charging curves verified this.

Two principal arrests were observed in the cathodic polarization curves. One arrest was at 1.05 v. and was present when the preceding anodic polarization was carried to 1.26 v. or 1.38 v., Figure 14, Curve A. This arrest probably corresponds to the electrochemical reduction of Au_2O_3 . Another arrest occurred at about 1.15 v. and is associated with an oxidation occurring after the oxidation at 1.38 v. has been completed, Figure 14, Curve B. Whether this oxidation product is a higher oxide of gold, a layer of oxygen chemisorbed on the Au_2O_3 , or some other species entirely has not been determined.

The quantity of electricity passed between 1.15 v. and the completion of the reduction beginning at 1.05 v. on cathodic polarization does not appear to depend on the quantity of electricity passed anodically between 1.26 v. and the oxygen evolution potential. The quantity of electricity passed in this region was usually around 8×10^{-4} coulombs irrespective of whether the reduction occurred in one or two steps. This is sufficient to reduce 1.7×10^{15} atoms of gold from the +3 to the zero oxidation state or 2.5×10^{15} atoms of gold from the +3 to the +1 oxidation state. From the value of the lattice parameter of gold, 4.07 \AA , and an assumed exposure of the (001) plane, it was calculated that there are 1.93×10^{15} atoms of gold at the surface of the electrode. The assumption was made in this

FIGURE 14 - CHARGING CURVES FOR GOLD



calculation that the real surface area is twice the apparent surface area, a value which is frequently used for shiny, noble metals (27). These calculations indicate that the oxide layer apparently did not penetrate beneath a monolayer of gold atoms in these experiments.

As far as the lower-valent oxides of gold are concerned, no definite proof of their existence has been found. The appearance of arrests in the portion of the anodic charging curve between 0.0 v. and 1.26 v. seemed to be dependent on the polarizing current density and the pretreatment of the electrode. At lower current densities, $12.5\text{--}72\text{ }\mu\text{a}/\text{cm}^2$, a brief arrest in the charging curve occurred anywhere from 0.4 v. to 0.9 v. Three curves, B, C, and D, which show the lower-potential region are given in Figure 8. The lower-potential breaks are best seen, however, in Curve A which illustrates the polarization of a gold electrode from which all oxides presumably have been removed by prolonged cathodic evolution of hydrogen. After the surface had been covered with an oxidized layer, the potential usually rose more rapidly to 1.26 v. on subsequent anodic polarizations. The anodic break occasionally seen in the neighborhood of 0.5 v. may be associated with the formation of Au_2O . The potential of the $\text{Au}/\text{Au}_2\text{O}$ couple has been reported by others as 0.36–0.42 v. (28). The slight anodic arrest in the neighborhood of 0.8–0.9 v. is in the region where the electrochemical

formation of a layer of chemisorbed oxygen (37) or possibly AuO (28) has been proposed by others.

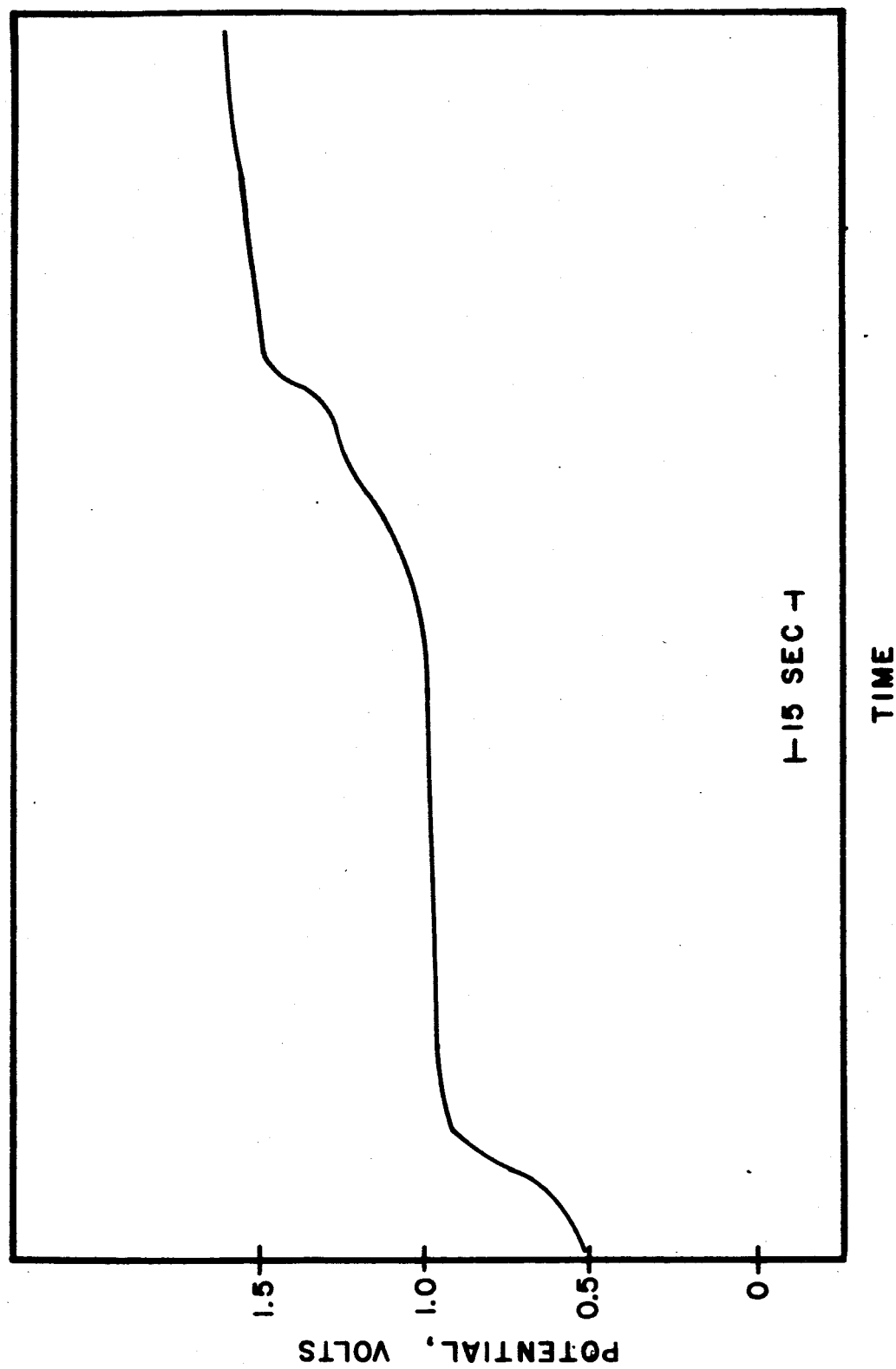
Cathodic charging at reduced current densities also may show additional depolarization steps. Two additional cathodic steps, at 0.8 and 0.3 v. were occasionally seen. The arrest at 0.3 v. has already been identified with the reduction of molecular oxygen; the step at 0.8 v. may be the reduction of a product (possibly AuO) formed at about the same potential anodically.

Anodic polarization indicated the formation of one principal oxide on palladium. This occurred between 0.89 v. and 0.94 v. on the typical anodic polarizations, Figure 7, Curve B, run after the electrode had absorbed hydrogen. On the initial anodic polarization, Curve A, the principal arrest was observed to be at 0.78 v. The slight drop in potential observed on initial polarizations of gold electrodes did not occur on palladium.

The principal oxide formed on palladium has been identified by others as PdO or $\text{Pd}(\text{OH})_2$. The standard potential for the Pd/PdO couple has been given as 0.79 v. (41) and 0.85 v. (39,40). Hence, the initial oxide arrest observed appears to be the formation of PdO or $\text{Pd}(\text{OH})_2$.

The region of oxide formation is shown in greater detail in Figure 15 where a slight indication of a break can be seen between 1.1 v. and 1.2 v. The potential then rises to 1.47 v. where a break leading to oxygen evolution occurs. These two additional potential arrests probably correspond

FIGURE 15 - CHARGING CURVE DETAIL FOR PALLADIUM



to the conversion of PdO to PdO_2 and palladium to PdO_2 . Hickling and Vrjosek (40) have suggested that the potential of the PdO/PdO_2 couple is 1.23 v. The potential of the Pd/PdO_2 couple has been measured by Hoare (41) as 1.47 v.

In addition to the long hydrogen ion discharge step beginning around 0.2 v., two other potential arrests were observed on the cathodic charging curve of palladium, Curve C, Figure 7. One, at about 0.665 v., is the reduction of PdO . The other cathodic arrest, occurring at 1.475 v., appears to be the reduction of a higher oxidation product, possibly PdO_2 .

In the oxide-formation region, behavior similar to that found on both palladium and gold electrodes was observed on most of the alloys. An anodic arrest around 1.26 v. was found on gold and all the alloys. This potential could be sustained for long periods of time with the appearance of oxygen and a gold-colored substance in the electrolyte. The mechanism for this reaction on the alloys is probably similar to that proposed for gold. On alloy electrodes containing forty or more percent palladium, an anodic arrest was also observed in the region of the Pd/PdO couple.

The potentials at which anodic arrests occurred are summarized in Table V. The potentials for the beginning of oxygen evolution, hydrogen ionization, and the anodic arrests occurring at lowered polarizing current densities are not shown in this table.

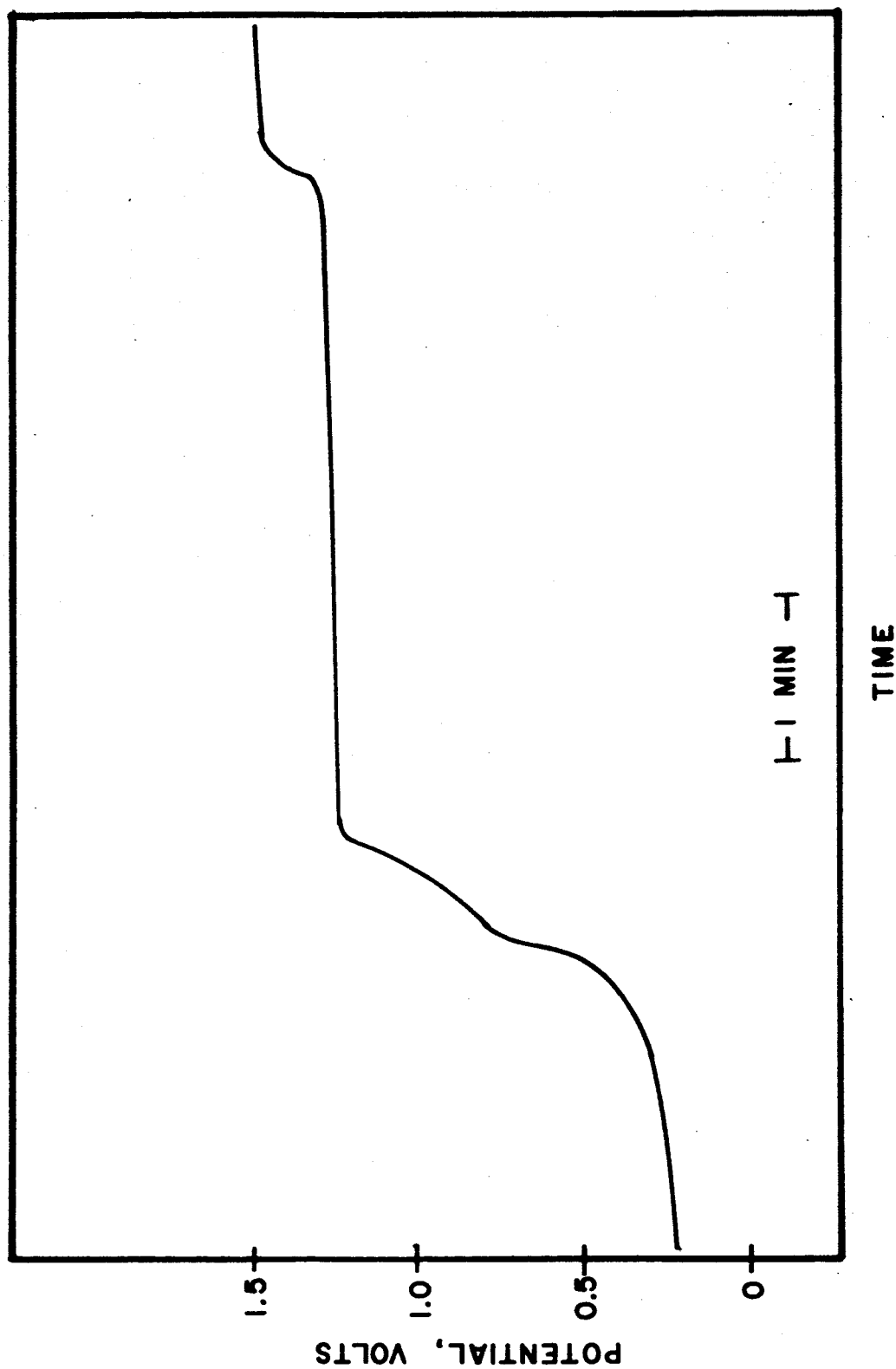
TABLE V

Potentials of Principal Anodic Arrests

Electrode	Potential			
Gold			1.26 v.	1.38 v.
80% Gold			1.27 v.	1.39 v.
75% Gold			1.24 v.	1.41 v.
60% Gold	0.54 v.	0.86 v.	1.26 v.	1.36 v.
40% Gold		0.90 v.	1.20 v.	
20% Gold		0.82 v.	1.24 v.	
Palladium		0.79 v.		

Anodic charging curves on the 20% gold electrodes show arrests in both the region of the PdO formation potential and the Au_2O_3 formation potential, Figure 16. On the initial anodic polarization, Figure 6, Curve A, when hydrogen was not present in the electrode and on polarizations run at low enough current densities such that most of the hydrogen was removed before the oxide formation began, Figure 16, the two anodic breaks occurred at 0.775-0.825 v. and 1.24 v. When the polarization was carried out at higher current densities, Curve B, Figure 6, the presence of hydrogen in the electrode appeared to force the oxide formation potentials to higher values.

FIGURE 16 - CHARGING CURVE DETAIL FOR 20% GOLD

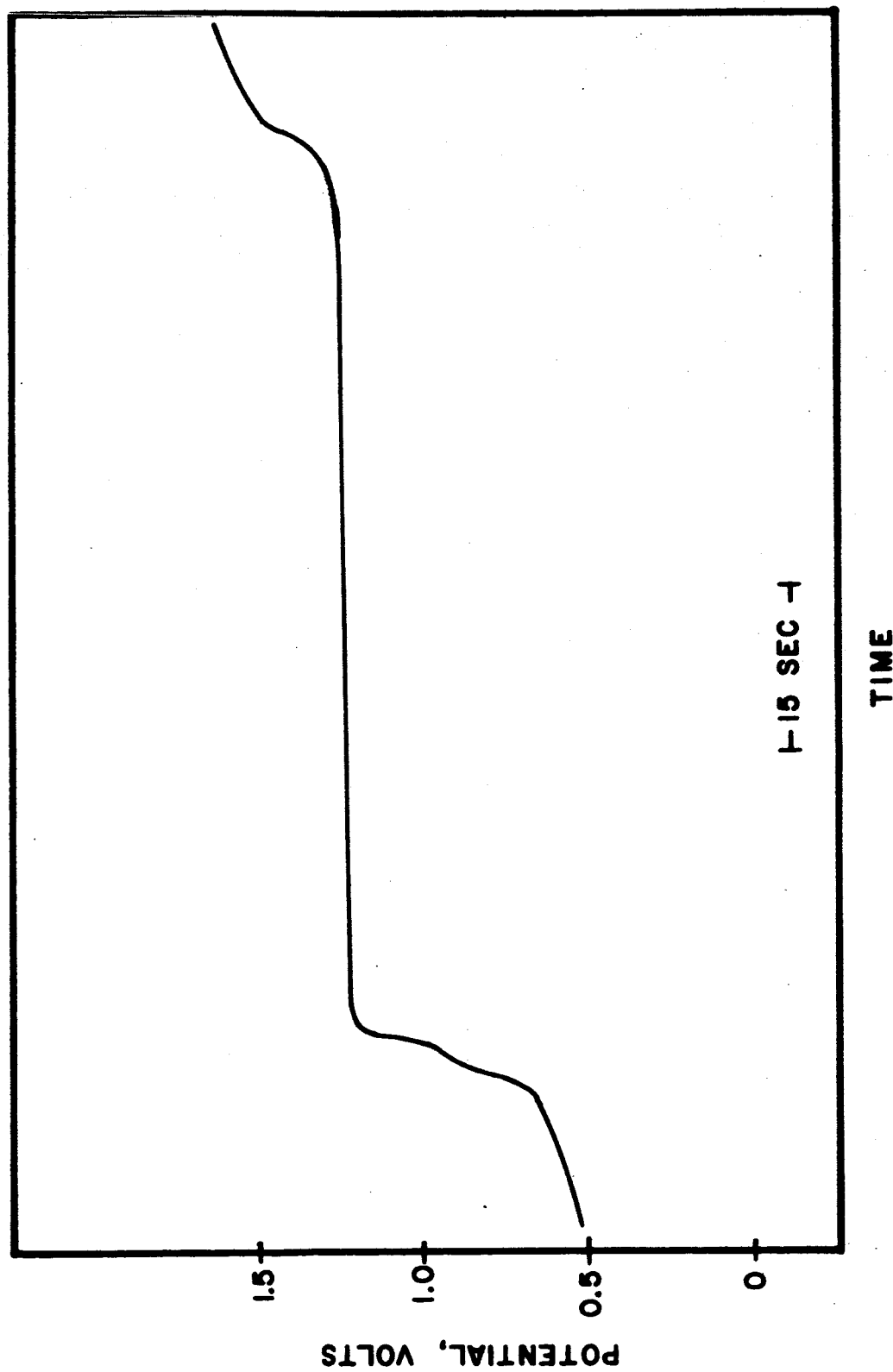


The potential of the higher anodic break, 1.24 v., has been sustained for 20 hours with the passage of oxygen and a gold-colored substance into the electrolyte. This reaction is apparently analogous to that occurring on gold electrodes at this potential.

Normally, with hydrogen in the 20% gold electrode, the potential dropped immediately from the oxygen-evolution potential to a value near the hydrogen-evolution potential on cathodic polarization. After the initial anodic polarization, when no hydrogen was present in the electrode, Curve C in Figure 6 was obtained on cathodic polarization. In addition to the hydrogen ion discharge step beginning at 0.225 v., two potential arrests are visible, one at 1.34 v. and one at 0.89 v. The potential-determining reactions on the cathodic charging curves were not identified.

The behavior of the 40% gold electrodes was very similar to that of the 20% gold electrodes. The two oxides appeared at about 0.9 v. and 1.2 v. on the typical anodic charging curves, Figure 17. On the initial anodic charging curve, Figure 5, Curve A, the first anodic arrest was very slight and the principal arrest occurred at a lower potential, 1.17 v. As with the 20% gold alloy, the presence of hydrogen in the electrode raised the potential of the anodic depolarization steps, Figure 5, Curve B. On both the initial and typical anodic charging curves another potential arrest was observed near 1.45 v. The

FIGURE 17 - CHARGING CURVE DETAIL FOR 40% GOLD

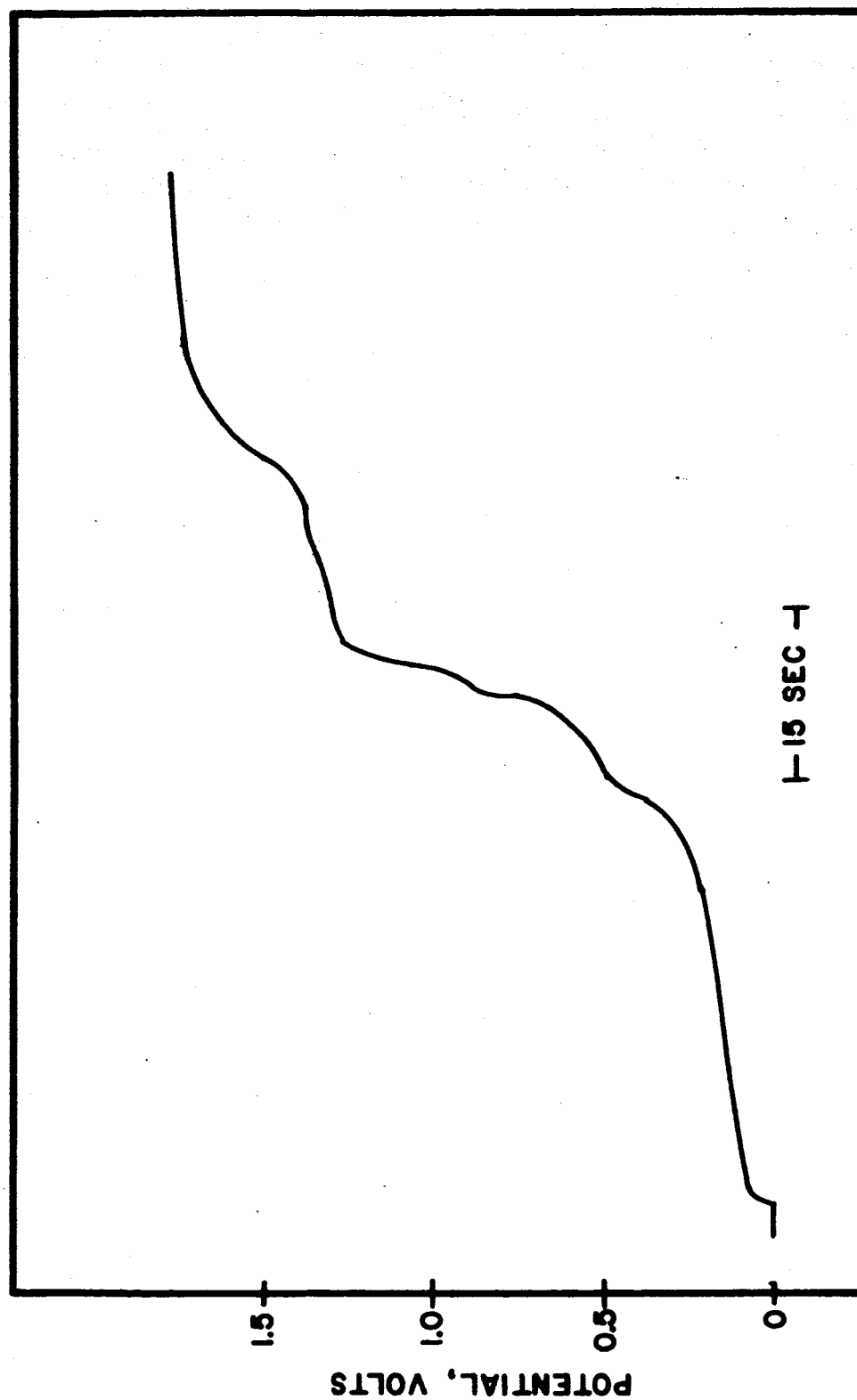


species responsible for this break may be similar to those involved in the Pd/PdO_2 couple which has a potential of 1.47 v.

In addition to the hydrogen ion discharge step beginning at 0.22 v., two other arrests were observed in the cathodic charging curve. One step, at 0.79 v., is associated with the reduction of the oxide formed at about 1.2 v., Curve C-2, Figure 5. The other cathodic arrest, at about 1.4 v., is associated with an oxidation product formed near oxygen evolution, Curve C-1, Figure 5.

The appearance of several oxides was observed on the anodic charging curves of 60% gold electrodes, Figure 18. Two anodic arrests similar to those found on gold were observed at 1.26 v. and 1.36 v. As with all the electrodes that absorb hydrogen, the presence of hydrogen in the electrode forced these arrests to somewhat higher values, Curve B, Figure 4. The break at 0.86 v., associated with a species presumably similar to PdO , was visible on most polarization curves. A fourth anodic arrest was prominent on this alloy. This arrest occurred around 0.5 v., Figure 18 and Figure 4, Curve B. A break at this potential was also observed occasionally on the 75% gold and 80% gold electrodes. It may be that the reaction responsible for this anodic arrest is the formation of a lower-valent oxide similar to Au_2O .

FIGURE 18 - CHARGING CURVE DETAIL FOR 60% GOLD



On the cathodic charging curve of the 60% gold alloy, Figure 4, Curve C, a broad region beginning at 1.1 v., in which several reductions took place, was observed. Three or more poorly-defined breaks were sometimes seen between 1.1 v. and 0.2 v. where hydrogen ion discharge began. In addition, when the anodic polarization had been carried to potentials near oxygen evolution, an arrest occurred at about 1.4 v. on cathodic charging. As with most other alloys, the potential-determining species on the cathodic charging curve were not identified.

The behavior of the 75% gold alloy was very similar to the behavior of the gold electrodes. Two arrests were observed in the anodic charging curve, Figure 3, Curve B. One arrest occurred at 1.41 v. and the other at 1.24 v. The depolarization process occurring at 1.24 v. has been sustained for up to 18 hours. As with gold, oxygen was produced and the electrolyte became gold-colored. It is likely that this behavior is typical of all the alloys. The additional anodic arrest at about 0.5 v., Figure 10, has already been discussed. An arrest around 0.84 v. was seen occasionally on the anodic polarization of the 75% gold electrodes. This arrest is in the region where formation of AuO (28) or a layer of chemisorbed oxygen (37) has been proposed for gold electrodes.

Cathodic charging curves for the 75% gold electrodes normally contained three steps, one at about 1.4 v. and one at about 1.2 v. both associated with reduction of an

oxidation product formed when the oxidation was carried above the potential of the principal oxide. Another cathodic arrest occurred at 0.74 v. and appeared to be associated with the oxidation at 1.26 v. A fourth cathodic arrest began at about 0.5 v. when oxygen was present in the electrolyte.

The electrochemical behavior of the 80% gold alloy, as illustrated in Figure 2, was very similar to the behavior of gold. The two principal anodic arrests occurred at 1.27 v. and 1.39 v. As with 75% gold electrodes, anodic arrests occasionally occurred around 0.3-0.4 v. and 0.8-0.9 v. The species responsible for these breaks have already been discussed. Two arrests were observed in the cathodic charging curve, Figure 2, Curve C. One was at about 1.3 v. and one at about 0.75 v.

SUMMARY OF RESULTS

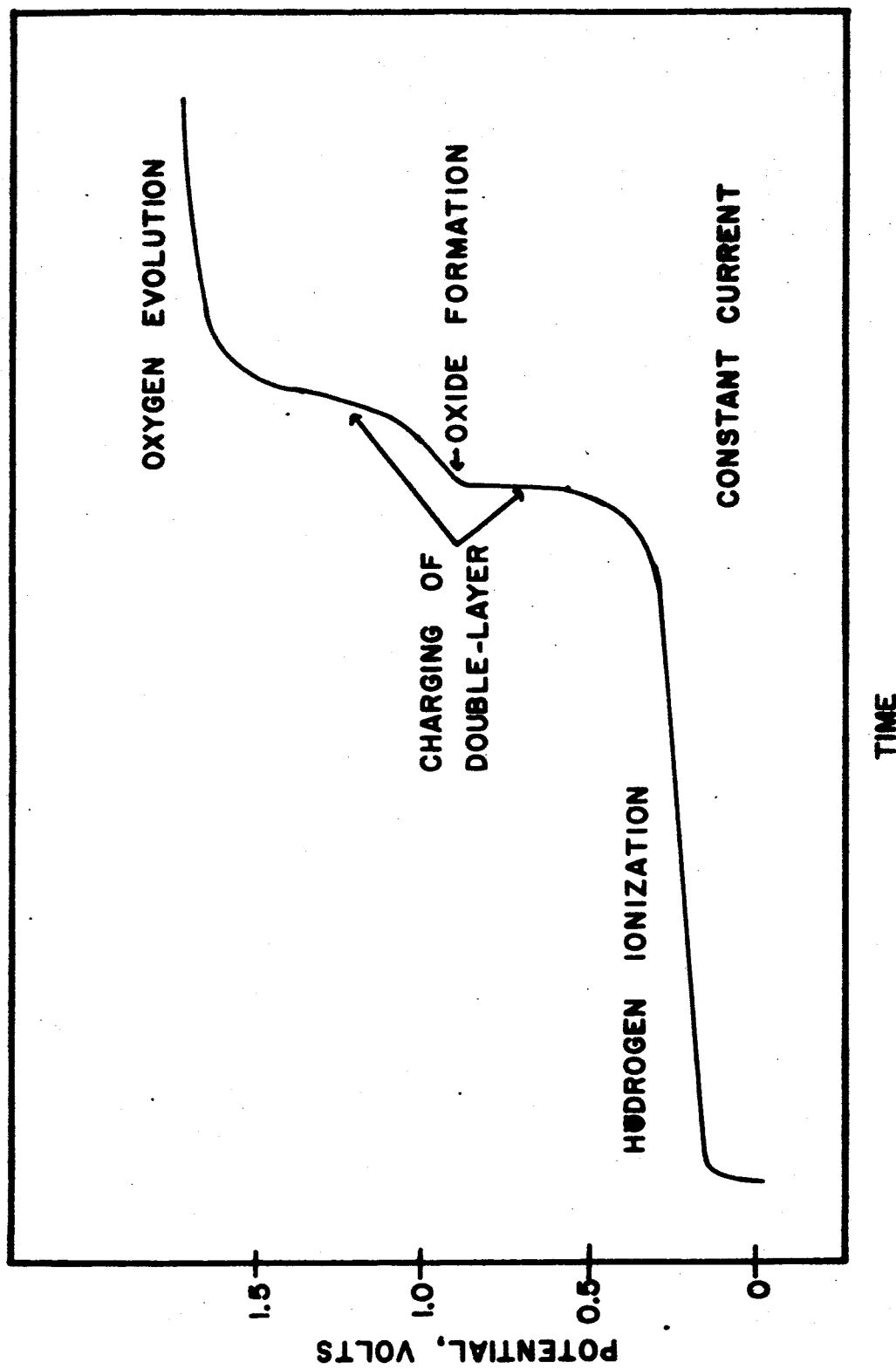
Palladium and the alloys with less than 75% gold were found to occlude hydrogen, while gold and alloys with 75 or more percent gold were not found to occlude hydrogen. Since it is at approximately 75% gold (62 atomic percent) that the d-band becomes full, it was concluded that unpaired d-electrons are necessary for exothermic occlusion of hydrogen. The rate of occlusion of hydrogen was found to be at a maximum at the 40% gold alloy and drop to zero at the 75% gold composition.

The alloys were all found to possess some characteristics of gold on anodic polarization. Each contained an anodic arrest near 1.26 v. This potential could be sustained for considerable periods of time with the passage of oxygen and a gold-colored substance into the electrolyte. The mechanism for this reaction on gold electrodes was proposed as the electrochemical formation of Au_2O_3 from a layer of oxygen chemisorbed on the gold electrode. The Au_2O_3 was proposed to decompose non-electrochemically to produce oxygen and regenerate the chemisorbed layer of oxygen on gold.

Electrodes with less than 75% gold were found to possess, in addition to the gold-like arrest, an anodic arrest in the region of the Pd/PdO potential. Cathodic polarization, however, indicated a palladium-like break on all the alloys.

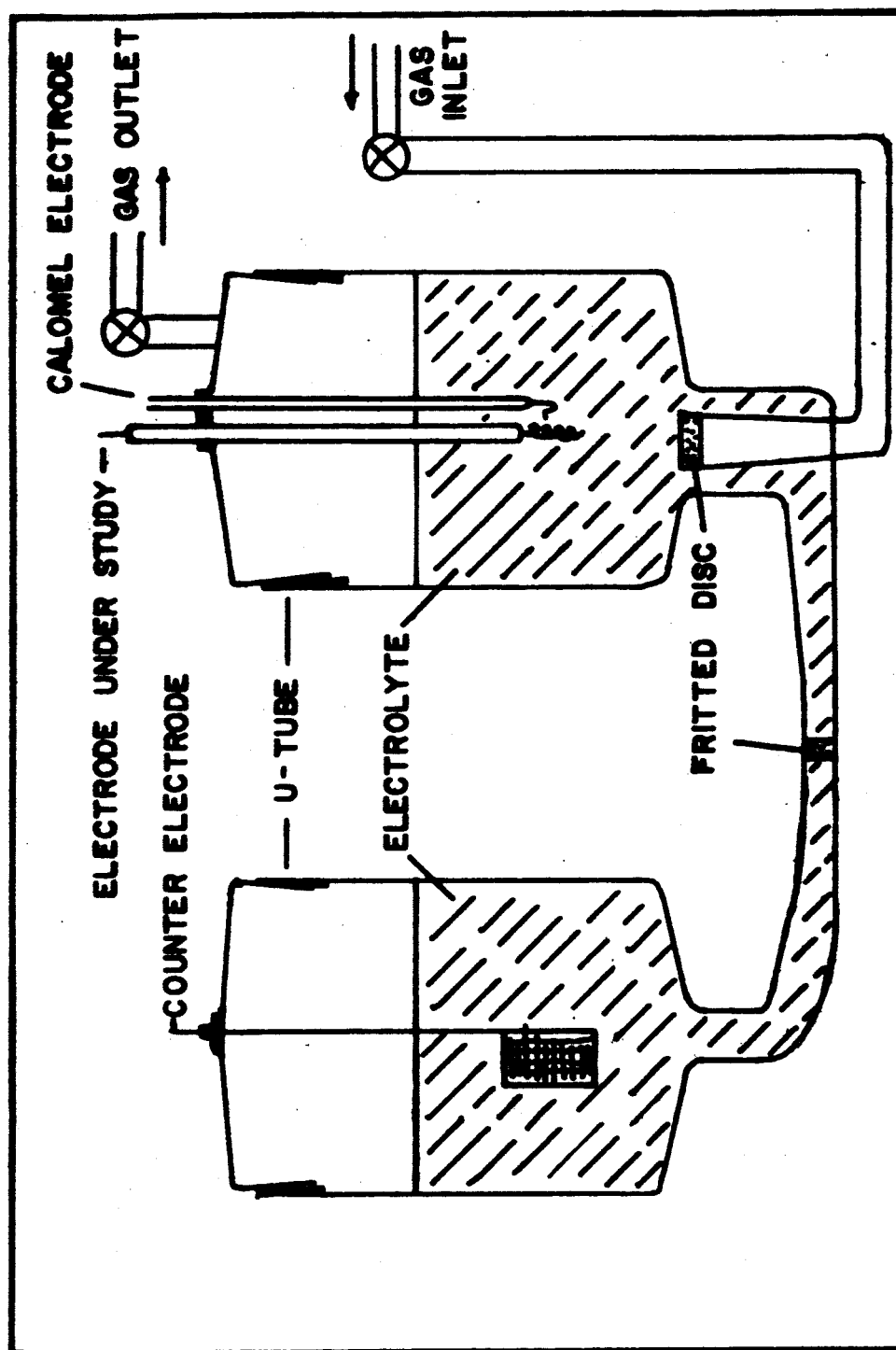
APPENDIX I

FIGURE 19 - TYPICAL ANODIC POLARIZATION CURVE



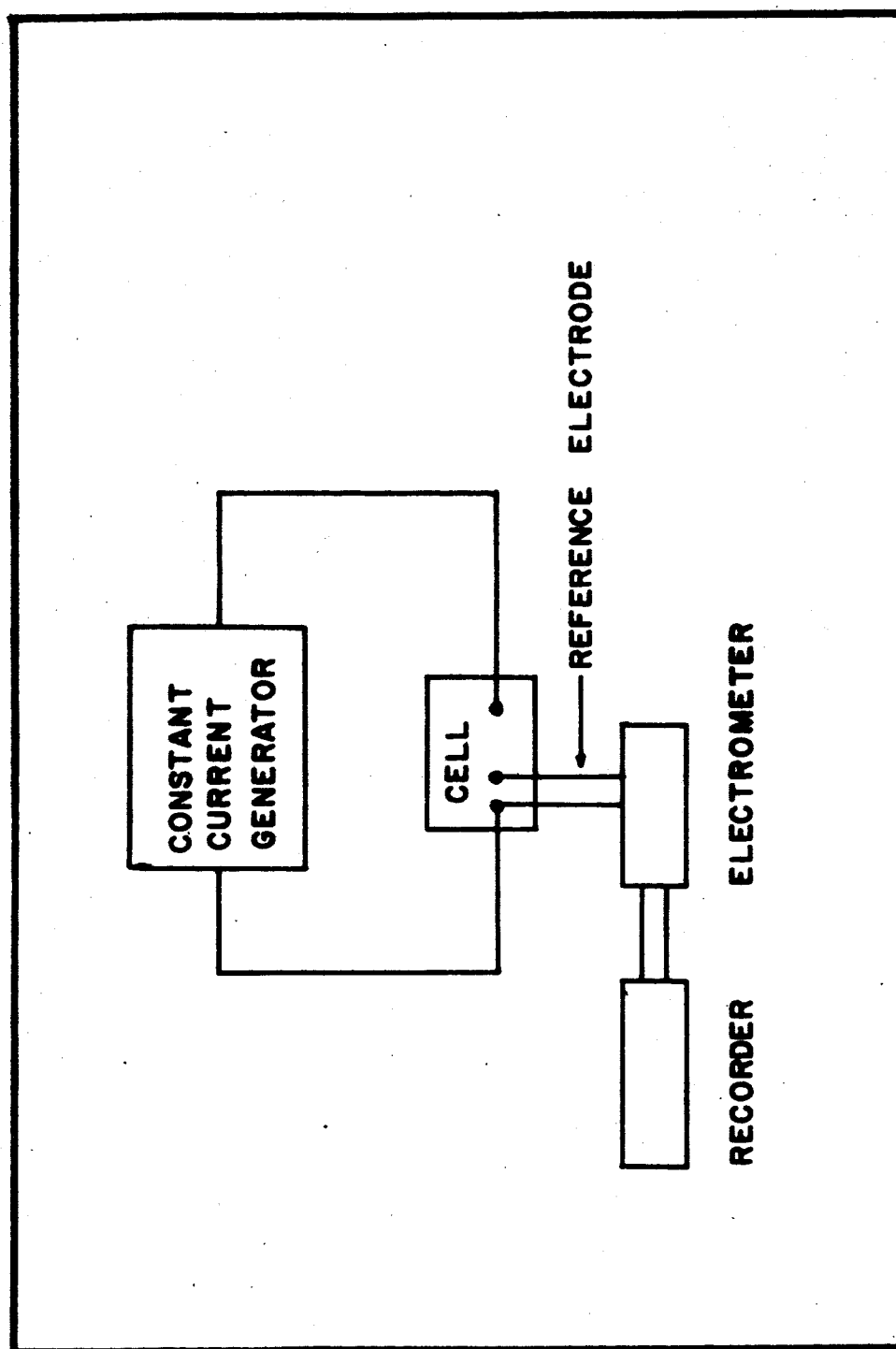
APPENDIX II

FIGURE 20- ELECTROLYTIC CELL



APPENDIX III

FIGURE 21 - ELECTRICAL MEASURING CIRCUIT



BIBLIOGRAPHY

- (1) D. O. Hayward and B. M. W. Trapnell, Chemisorption, 2nd edition, p. 231. Butterworths, Washington (1964).
- (2) *ibid.*, p.232.
- (3) R. E. Norberg, *Phys. Revs.*, 86, 745 (1952).
- (4) Handbook of Chemistry and Physics, 43rd edition, pp. 2734, 2736. Chemical Rubber Publishing Co., Cleveland (1961).
- (5) G. C. Bond, Catalysis by Metals, p. 25. Academic Press, New York (1962).
- (6) N. F. Mott and H. Jones, The Theory of the Properties of Metals and Alloys, p. 199. Dover Publications, Inc., New York (1958).
- (7) P. Delahay, New Instrumental Methods in Electrochemistry, p. 181. Interscience Publishers, Inc., New York (1954).
- (8) E. C. Potter, Electrochemistry, Principles and Applications, p. 164. The Macmillan Company, New York (1956).
- (9) *ibid.*, p. 166.
- (10) D. P. Smith, Hydrogen in Metals, The University of Chicago Press, Chicago (1948).
- (11) *ibid.*, p. 85.
- (12) J. P. Hoare and S. Schuldiner, *J. Phys. Chem.*, 61, 399 (1957).

- (13) T. B. Flanagan and F. A. Lewis, J. Chem. Phys., 29 1417 (1958).
- (14) C. P. Aben and W. G. Burgers, Trans. Faraday Soc., 58, 1989 (1962).
- (15) R. E. Norberg, Phys. Revs., 86, 745 (1952).
- (16) D. P. Smith, loc. cit., p. 191.
- (17) D. J. G. Ives and S. Swaroopa, J. Chem. Soc., 3489 (1955).
- (18) A. J. Berry, J. Chem. Soc., 99, 463.
- (19) A. Sieverts, E. Jurisch, and A. Metz, Z. anorg. allgem. Chem., 92, 329 (1915).
- (20) T. B. Flanagan and A. Maeland, Abstracts of 148th Meeting of American Chemical Society, p. 12 v. (1964).
- (21) J. Benard and J. Talbot. Compt. Rend., 222, 493 (1946).
- (22) H. Mundt, Ann. Physik, 19, 721 (1934).
- (23) J. P. Hoare, G. W. Castellan, and S. Schuldiner, J. Phys. Chem., 62, 1141 (1958).
- (24) F. H. Jeffery, Trans. Faraday Soc. (1915). Chem. Abs., 10, 150 (1916).
- (25) F. Jirsa and O. Buryanek, Z. Elektrochem., 29, 126 (1923).
- (26) G. Armstrong, F. R. Himsworth, and J. A. V. Butler, Proc. Roy. Soc., A143, 89 (1933).
- (27) A. Hickling, Trans. Faraday Soc., 42, 518 (1946).
- (28) S. E. S. El Wakkad and A. M. Shams El Din, J. Chem. Soc., 3089 (1954).

- (29) J. K. Lee, R. N. Adams, and C. E. Bricker, *Anal. Chim. Acta*, 17, 321 (1957).
- (30) K. J. Vetter and D. Berndt, *Z. Elektrochem.*, 62, 378 (1958).
- (31) S. Barnartt, *J. Electrochem. Soc.*, 106, 722 (1959).
- (32) S. B. Brummer and A. C. Makrides, *J. Electrochem. Soc.*, 111, 1122 (1964).
- (33) G. M. Schmid and R. N. O'Brien, *J. Electrochem. Soc.*, 111, 832 (1964).
- (34) G. Deborin and B. Ershler, *Acta Physicochim.*, 13, 347 (1940).
- (35) D. Clark, T. Dickinson, and W. N. Mair, *Trans. Faraday Soc.*, 55, 1937 (1959).
- (36) H. A. Laitinen and M. S. Chao, *J. Electrochem. Soc.*, 108, 726 (1961).
- (37) J. P. Hoare, *J. Electrochem. Soc.*, 110, 245 (1963).
- (38) J. A. V. Butler and G. Drever, *Trans. Faraday Soc.*, 32, 427 (1936).
- (39) S. E. S. El Wakkad and A. M. Shams El Din, *J. Chem. Soc.*, 3094 (1954).
- (40) A. Hickling and G. G. Vrjosek, *Trans. Faraday Soc.*, 57, 123 (1961).
- (41) J. P. Hoare, *J. Electrochem. Soc.*, 111, 610 (1964).
- (42) J. J. MacDonald and B. E. Conway, *Proc. Roy. Soc.*, A269, 419 (1962).
- (43) L. Nowack, *Z. anorg. allgem. Chem.*, 113, 1 (1920).
- (44) A. Couper and D. D. Eley, *Discuss. Faraday Soc.*, 8, 172 (1950).
- (45) W. K. Hall and P. H. Emmett, *J. Phys. Chem.*, 62, 816 (1958).